Toxicology International, *31(3) : 489-513; 2024. DOI: 10.18311/ti/2024/v31i3/43658*

Online ISSN : 0976-5131; Print ISSN : 0971-6580

Toxicology International

Contents available at: www.informaticsjournals.com/index.php/toxi



Therapeutic Potential of *Curcuma longa* Rhizome Solvent Fractions Against Benz[a]Anthracene-induced Pulmonary Toxicity: *In vivo* Insights

Oladipo Miriam Oluchi[1*], Nwankwo Henry Chukwuebuka[1], Imotor Isaac Ieren[1], Oladipo Bamidele Fatai[2], Bosha A. Joel[1], Saganuwan Alhaji Saganuwan[1] and Onyeyili Patrick Azubuike[1]

[1]Department of Veterinary Pharmacology and Toxicology, University of Agriculture, Makurdi. P. M. B. 2373 Makurdi, Benue, Nigeria; mimsonex@gmail.com

[2]Del Scan Services Limited. 12th, 7th Avenue off Inikpi Street, High Level, 970001 Makurdi, Benue State, Nigeria

Abstract

Benz[a]anthracene, a polycyclic aromatic hydrocarbon found in environmental pollutants, poses significant health risks, particularly to the respiratory system. This study aimed to evaluate the potential therapeutic effects of different solvent fractions of *Curcuma longa* rhizome methanol extracts against benz[a]anthracene-induced pulmonary toxicity using an *in vivo* rat model. The methanol crude extract of *C. longa* was partially fractionated using partition chromatography with silica gel as the adsorbent. Four solvent fractions obtained using gradient elution (designated ethanol, ethyl acetate, diethyl ether, and n-hexane fractions) were collected and used in the experiment. Albino Wistar rats (*Rattus norvegicus*) were randomly divided into seven groups and administered benz[a]anthracene to induce pulmonary toxicity. Subsequently, rats were treated with different solvent fractions of *C. longa* or diclofenac sodium as a positive control. Body weights were measured weekly, pre-induction, post-induction and post-treatment blood samples were collected, and lung tissue samples were collected and analysed. Treatment with the ethyl acetate fraction of *C. longa* resulted in significant improvements in lung histopathology compared to benz[a]anthracene-treated rats alone, suggesting potential anti-inflammatory effects. Furthermore, this fraction showed significant antioxidant enzyme activities, including glutathione peroxidase, glutathione reductase, and superoxide dismutase, indicating its ability to mitigate oxidative stress. Biochemical analysis revealed that the ethyl acetate fraction also significantly decreased serum levels of tumour biomarkers, such as epidermal growth factor receptor, cancer antigen 125, and carcinoembryonic antigen, suggesting its potential in inhibiting cancer-related processes induced by benz[a]anthracene exposure. Our findings suggest that the ethyl acetate fraction of *C. longa* rhizome may hold promise as a therapeutic agent against benz[a]anthracene-induced pulmonary toxicity, possibly through its anti-inflammatory, antioxidant, and anticancer properties. Further research is warranted to elucidate the specific compounds present in this fraction and the underlying mechanisms through which they exert their effects, to optimize their therapeutic potential.

Keywords: Benz[a]anthracene, *Curcuma longa*, Histopathology Scoring, Pulmonary Toxicity, Rats

**Author for correspondence*

Article Received on: 17.04.2024 Revised on: 25.06.2024 Accepted on: 26.06.2024

1. Introduction

Benz[a]anthracene, a polycyclic aromatic hydrocarbon found in various environmental pollutants, is well-known for its carcinogenic properties and adverse effects on pulmonary health. Benz[a]anthracene is classified as hazardous on the right-to-know list and the special health hazard substance list[1]. It is present in coal tar, roasted coffee, smoked foods, and automobile exhaust, and is produced as an intermediate during chemical manufacturing. Consequently, it possesses the potential to inflict more harm than currently acknowledged[1]. Human exposure to Benz[a]anthracene and other PAHs occurs primarily through ingestion and inhalation from smoking or second-hand smoke, air pollution with combustion products, or thermal processes in food preparation (such as grilling and roasting) and water pollution with combustion products and may occur through bioaccumulation of benz[a]anthracene in consumed animals, such as livestock, and also by polluted air through exposure to exhaust fumes from burning fossil fuel[2-4]. Oral exposure to benz[a]anthracene in rats induced dose-dependent gross and histopathological damage to the lung showing inflammatory responses and tissue damage in the lungs, such as congestion and damaged alveolar sacs with cellular infiltration[5]. In recent years, there has been growing interest in exploring natural compounds with potential therapeutic benefits in mitigating environmental carcinogen (such as benz[a] anthracene)-induced lung injury.

Curcuma longa, commonly known as turmeric, has been widely studied for its pharmacological properties, including anti-inflammatory, antioxidant, and anticancer effects, and various pharmacological activities[6-8]. The rhizome of *C. longa* contains diverse bioactive compounds, such as curcuminoids, turmerones, and flavonoids, which have been shown to possess therapeutic potential in various disease conditions[9-12]. However, the efficacy of different solvent fractions of *C. longa* rhizome in mitigating environmental carcinogen (such as benz[a] anthracene)-induced pulmonary toxicity has not been extensively investigated.

This study aimed to evaluate the potential therapeutic effects of different solvent fractions of the methanol crude extract of *C. longa* rhizome against benz[a] anthracene-induced pulmonary toxicity using an *in vivo* rat (*Rattus norvegicus*) model. We assessed the impact of these fractions on various parameters, including lung histopathology, antioxidant enzyme activities, serum biomarkers of inflammation and oxidative stress, as well as haematological and oncogenic parameters.

2. Method

2.1 Partial Purification of Crude Extract of *Curcuma longa* (Partition Chromatography)

The partial purification of the methanol crude extract of *C. longa* was done using a modified method of Malwade *et al.*[13] The crude extract was separated using silica gel (as adsorbent, 70-230 mesh) packed in a chromatographic column. The adsorbent was overlaid with cotton wool before and after plant extract application. This is to prevent direct contact or mixing of the extract with the silica gel, to absorb shock (that may cause a crack in the loaded adsorbent) when the solvent is poured into the chromatographic column, and to serve as a filter for particles that may lurk within the solvent. A slurry of finely powdered silica gel (in hexane) was packed in a glass column (50 cm) to a height of about 12 cm (and a diameter of 3 cm). The column was conditioned with 100% n-hexane and the gradient started with 100% n-hexane followed by a 10% stepwise gradient from 100% n-hexane to 100% diethyl ether, to 100% ethyl acetate, and 100% ethanol. Hundred (100) mL of each solvent fraction were collected. The fractions were allowed to dry at room temperature and stored at 4°C. The quantity yield was calculated using the formula below.

$$Yield(g) = Weight\ of\ dried\ mass\ with\ container - Weight\ of\ empty\ container$$

2.2 Experimental Animals

Breeding rats (*Rattus norvegicus* also called Wistar rats) were sourced from local breeders in Makurdi, Benue state, Nigeria. They were kept in plastic cages in a room maintained at 25±2 °C with a 12h light/dark cycle. The animals used for the experiment were bred and allowed to attain maturity (8 to 12 weeks old) before they were employed for the experiment. They were fed with standard feeds (Chikun grower(R) pellet) and water was provided *ad libitum*. The experiment was conducted according to international guiding principles for biomedical research involving animals[14], and as recommended by the ethical

committee of the College of Veterinary Medicine, Joseph Sarwuan Tarka University, Makurdi; with designated ethical clearance reference number JOSTUM/CVM/ETHICS/2023(2).

2.3 Ameliorative Potentials of the Different Solvent Fractions of *Curcuma longa Linn* Rhizome in Benz[A]Anthracene-Induced Toxicity in Rats

The rats weighing an average of 80.2 g were randomly divided into seven (7) groups of six (6) rats each and marked with picric acid stain for easy identification. Group one (I) rats were administered only water, all other groups (Group II to VII) were treated by gavage with 50 mg/kg body weight of 10 mg/ml Benz[a]anthracene in 5% DMSO for 21 days. After blood samples were collected; Groups III, IV, V, and VI rats were treated by gavage with 25 mg/kg body weight/day of 10 mg/mL different solvent fractions of the methanol extract of *C. longa* rhizome (ethanol fraction, ethylacetate fraction, diethyl ether fraction, and hexane fraction respectively) for another 21 days. Group VII rats were treated with 10 mg/kg body weight/day of 20 mg/mL diclofenac sodium as the positive control group. Three (3) of Group II rats were selected at random and euthanized while the other 3 rats were left untreated after the induction till the end of the study. The body weights of the rats were measured and recorded weekly. Pre-induction, post-induction and post-treatment blood samples were collected for analysis through the retro-orbital sinus route[15] and divided into two separate well-labelled sample tubes (plain tubes and anticoagulated tubes). Anticoagulated blood samples were used for haematological parameters which include Packed Cell Volume (PCV), Red Blood Cell (RBC) count, and total and differential White Blood Cell (WBC) count as described by Cheesbrough, Wayne, Pal, Wayne, Chabot-Richards, and George, respectively[16-20]. Serum was harvested from the whole blood sample in the plain tubes for biochemical analysis such as liver and renal function tests (the colourimetric method was applied accordingly), and tumour biomarkers such as Epidermal Growth Factor Receptor (EGFR), Cytokeratin Fragment Antigen 21-1 (CYFRA 21-1), Cancer Antigen 125 (CA-125), and Carcinoembryonic Antigen (CEA) (using the ELISA principle). Animals were euthanized after the collection of post-treatment blood samples using 100 mg/kg pentobarbital[21]. The lungs were excised quickly and weighed after the animals were euthanized. One lung tissue was washed in a chilled wash buffer, diced into smaller pieces, and placed in an ice-cold homogenizing buffer at a 1:10 ratio[22]. The lung tissues were homogenized using a glass-teflon homogenizer (PT 1600 E, kinematica AG, dispensing and mixing technology). The homogenates were was poured into a glass tube on ice and centrifuged at 10,000g for 10-20 min at 4°C. Debris and particulate matter were removed and the Post-Mitochondrial Supernatant (PMS) was obtained and shared into aliquots in a well-labeled Eppendorf and stored at -20°C until used. This sample was used for the analysis of tissue antioxidants such as reduced Glutathione (GSH), Glutathione –S- Transferase (GST), Glutathione Reductase (GR), Glutathione Peroxidase (GPx), catalase, Superoxide Dismutase (SOD), and tissue protein as described by Jollow *et al.*, Habig *et al.*, Carlberg and Mannervik, Mohandas *et al.*, Claiborne, Beauchamp and Fridovich, and Bradford, respectively[23-29]. The second piece of the lung tissues were fixed in 10% buffered formalin for histopathology assessment[30]. The lesions observed were photographed using a Magnus digital pad microscope camera. All the tissue slides were examined blindly, and the occurrence of lesions in the organ was assessed according to the methodology proposed by Giordani *et al.*[31]

2.4 Assessment and Scoring Guide of the Lung Histopathological Picture

In our study, we assessed lung histopathological images to evaluate the degree of pulmonary toxicity induced by Benz[a]anthracene and the potential therapeutic effects of *C. longa* rhizome fractions. We modified and simplified the histopathological scoring methods of Ashcroft *et al.*, Hübner *et al.*, Kubiak *et al.*, and Silva *et al.*, to ensure clarity and ease of use[32-35].

We considered the following parameters for scoring:

The data collected were organised using the Microsoft Excel sheet. The data collected were composed mainly of low values (such as zero), formal normality testing was not feasible. Therefore, we used the median score for each parameter for further analysis[36], this approach also helps to mitigate the potential impact of outliers.

Percentage damage was calculated using the median score for each parameter, divided by the maximum allocated score for that parameter, multiplied by 100. The maximum score per scanned slide was 40.

Parameter	Description	Score Range	Legends
Atelectasis	Lung alveolar deflation causing partial or complete collapse	0, 1, 2, 3, 4	0: No atelectasis 1: 1/4 of lung affected 2: 1/2 of lung affected 3: 3/4 of lung affected 4: Entire lung affected
Hemorrhage	Presence of erythrocytes within alveolar lumens or interstitium	0, 1, 2, 3, 4	0: No hemorrhage 1: 1/4 of lung affected 2: 1/2 of lung affected 3: 3/4 of lung affected 4: Entire lung affected
Vessel Congestion	Degree of alveolar capillary congestion	0, 1, 2, 3, 4	0: No congested capillaries 1: Congestion in one quadrant 2: Congestion in two quadrants 3: Congestion in three quadrants 4: Congestion in all quadrants
Alveolar Wall Thickness	Thickness exceeding one cell	0-16	Ranging from 0 (1 cell thickness in 2/3 of the histopathology picture) to 16 (more than 4 cell thickness in the entire lung histopathology picture)
Cellular Infiltration	Presence of wandering cells in air and interstitial spaces	0, 1, 2, 3, 4	0: Less than 10 cells 1: At least 10 cells 2: At least 25 cells 3: At least 50 cells 4: Over 75 cells
Inflammatory Cells	Presence of inflammatory cells in tissue and air spaces	0, 1, 2, 3, 4	0: Less than 10 cells 1: At least 10 cells 2: At least 25 cells 3: At least 50 cells 4: Over 75 cells
Enhanced Injury	Overall impression of tissue-level injury	0, 1, 2, 3, 4	0: No injury 1: Mild loss (1/4 of lung tissue) 2: Moderate loss (1/2 of lung tissue) 3: Severe loss (3/4 of lung tissue) 4: Complete loss (entire lung tissue)

Percentage damage is calculated using the median score of each parameter using by the formula

$$\left(\frac{median\,score}{Maximum\,allocated\,score\,of\,the\,parameter}\times 100\right)$$

The maximum score per scanned slide is 40. The total score is then transformed to a range of 0 – 100 using the formula

$$\left(\frac{Sum\,of\,median\,score\,of\,all\,the\,parameters\,per\,slide}{40}\times 100\right).$$

This methodology simplifies the assessment and scoring process, making it accessible for researchers and ensuring consistent and reliable data analysis across experimental groups.

2.5 Statistical Analysis

All data generated during the study were expressed as mean ± Standard Error of the Mean (S.E.M) and analyzed statistically by both one-way and two-way Analysis of Variance (ANOVA), depending on the available variables. Significant differences were considered at $p < 0.05$ using the Post Hoc Tukey test. Data were analyzed using GraphPad Prism 9 computer statistical software[37]. Values are then compared between and across all the experimental groups.

3. Result

3.1 The Partial Purification Yield of Different Solvent Fractions of *Curcuma longa*

The yield of different solvent fractions of *C. longa* is presented in Table 1. The Ethyl Acetate Fraction (EAF) had the highest yield (0.176g) while the Ethanol Fraction (ETF) had the lowest yield (0.081g).

3.2 Effects of Different Solvent Fractions of *Curcuma longa* on Body Weights of Rats Exposed to Benz[a]anthracene

The effect of benz[a]anthracene oral administration on the body weight of Wistar rats was more evident after one week of administration. Significant (p<.05) weight loss was observed at day 14 and 21 across the entire experiment groups when compared to day 0 (pre-induction) except that of the control group where the average percentage change in body weight was significantly increased at day 14 (61.19%) and, day 21 (73.11%) (Table 2). One week after the commencement of treatment (day 28), the body weight recovery was significant (p<.05) in the Ethanol Fraction (ETF), Ethyl Acetate Fraction (ETF), and *n*-Hexane Fraction (HXF) treated groups with an average percentage weight gain of 66.47%, 63.58%, and 68.91% respectively when compared to that of day 21 (end of induction) values (55.18%, 49.00%, and 55.39% respectively). There was no significant difference (p>.05) when these values were compared to the average percentage weight gain of the control (91.13%) group.

At the end of the study (day 42), there were significant (p<.05) improvements in the body weights when compared to post-induction values across all the treatment groups except with the benz[a]anthracene group. The post-treatment (day 42) average percentage weight gain of the benz[a]anthracene group (60.50%) was not significant (p>.05) when compared to the post-induction (day 21) value (50.76%). This value was also significantly decreased (p<.05) when compared to that of the post-treatment weight gain of the control group (159.30%). There was significant weight gain (p<.05) in the control group, throughout the study. The highest weight gain was observed with the EAF-treated group at week 2/day 35 (92.39%) and week 3/day 42 (111.51%) of the treatment. This weight gain was significant (p<.05) when compared to its post-induction/day 21 average percentage body weight (49.00%). There was also

no significant difference (p>.05) in the change in body weight across the column when compared to each other (Table 2).

The post-mortem lung weight of EAF (1.79±0.14g) and Diethyl Acetate Fraction (DEF) (1.64±0.14g) were significantly increased (p<.05) when compared to the control (0.98±0.05g) group. The value of the lung/body weight ratio of the rats' lungs showed a significant increase (p<.05) in the benz[a]anthracene (1.18±0.11%), EAF (0.97±0.04%) and, DEF (0.95±0.02%) treated groups when compared to the control (0.62±0.04%) group (Table 3).

Table 1. Yield from different solvents of the methanol extract of *C. longa* rhizome

Solvent Fraction	Yield (g)
Ethanol	0.081
Ethyl acetate	0.176
Diethyl ether	0.101
***n*-Hexane**	0.115

3.3 Effects of Different Solvent Fractions of *Curcuma longa* Rhizome on the Serum Biochemical Parameters of Rats Exposed to Benz[a]anthracene

The difference between the pre-induction and post-induction serum levels of AST, ALT, urea, and creatinine were not significant (p>.05) following the administration of 25 mg/Kg/bw/day of benz[a]anthracene. There was a significant decrease (p<.05) in the post-treatment AST levels of ETF (168.85±7.45 U/L), EAF (212.87±15.96 U/L), DEF (193.63±8.48 U/L), and HXF (218.85±11.57 U/L) when compared to their pre-induction AST levels (275.45±5.62, 270.01±5.84, 270.82±12.17, and 275.23±8.39 U/L respectively). The post-treatment AST levels of ETF, EAF, and DEF were significantly decreased when compared to their post-induction AST values (275.52±22.2, 318.05±29.43 and, 312.48±8.35 U/L respectively). The post-treatment AST levels of EAF, and DEF were significantly lower (p<.05) than the AST value (313.84±51.84 U/L) of the benz[a]anthracene group (Table 4). The post-treatment AST levels of the benz[a]anthracene group remained significantly increased (p<.05) when compared to their pre-induction levels (255.72±22.96 U/L) 21 days after induction was stopped.

Table 2. Mean*Body weight of Wistar rats treated with *C. longa* methanol extract fractions after benz[a]anthracene exposure

	Body weight of treatment groups (g) (percentage change in body weight)						
Days	**Control**	**Benz[a] anthracene (25mg/kg)**	**Benz[a] anthracene + Ethanol fraction (25mg/kg)**	**Benz[a] anthracene + Ethylacetate fraction (25mg/kg)**	**Benz[a] anthracene + Diethyl ether fraction (25mg/kg)**	**Benz[a] anthracene + *n*-Hexane fraction (25mg/kg)**	**Benz[a] anthracene + Diclofenac Na(10mg/kg)**
0 (Pre-induction)	62.43±0.84	92.93±9.09	75.38±1.32	86.03±5.32	87.55±4.27	79.17±2.90	82.77±4.09
7 (During induction)	80.93±2.63[a] (29.52)	113.28±9.33[a] (22.65)	110.07±6.14[a] (46.43)	116.25±5.94[a] (35.94)	116.03±5.95[a] (32.88)	114.15±4.42[a] (45.30)	100.13±5.21 (22.31)
14 (During induction)	100.72±7.46[a] (61.19)[c]	119.40±11.22 (30.01)	111.87±8.32 (49.19)	120.92±5.38 (41.71)	126.02±5.14 (47.04)	118.20±3.99 (49.84)	103.18±7.46 (26.93)
21 (End of induction)	108.15±7.14[a] (73.11)[c]	135.47±10.93 (50.79)[b]	116.62±6.16 (55.18)	127.48±5.52 (49.00)	129.03±7.99 (46.01)	122.85±4.89 (55.39)	106.57±4.74 (30.84)
28 (During treatment)	119.32±7.45 (91.13)	135.91±8.67 (51.01)[b]	129.62±6.33[a] (66.47)[d]	140.30±4.42 (63.58)[d]	136.10±11.59 (50.28)	131.39±5.57[a] (68.91)[d]	118.10±8.57 (43.64)
35 (During treatment)	140.82±9.92[a] (125.70)[d]	140.87±10.64 (56.07)[b]	144.74±6.9[a] (84.93)[d]	168.20±6.38[a] (92.39)[d]	155.53±13.35[a] (66.15)	141.70±5.91 (78.66)[d]	137.04±13.11[a] (58.59)
42 (End of treatment)	161.62±11.34[a] (159.30)[d]	145.04±10.25 (60.50)[b]	159.74±6.61[a] (101.20)[d]	183.18±7.73[a] (111.51)[d]	172.52±16.59[a] (76.47)	154.02±5.85[a] (89.38)[d]	148.79±12.71[a] (72.16)[d]

a = Significant increase when compared to the previous body weight (p<.05)
b = Significant decrease in percentage change in weight when compared to the control group (p<.05)
c = Significant increase in percentage change in weight when compared to day 7 (p<.05)
d = Significant increase in percentage change in weight when compared to day 21 (p<.05
*Mean ± SEM of 6 observations

Table 3. Mean* weight and lung/body weight ratio of the lungs of Wistar rats treated with *C. longa* methanol extract fractions after benz[a]anthracene exposure

	Treatment groups						
Parameters	**Control**	**B[a]A (25mg/kg)**	**B[a]A + Ethanol fraction (25mg/kg)**	**B[a]A + Ethylacetate fraction (25mg/kg)**	**B[a]A + Diethyl ether fraction (25mg/kg)**	**B[a]A + *n*-Hexane fraction (25mg/kg)**	**B[a]A + Diclofenac Na (10mg/kg)**
Lung weight (g)	0.98±0.05	1.69±0.21	1.11±0.08	1.79±0.14[a]	1.64±0.14[a]	1.40±0.10	1.60±0.17
Lung weight/ body weight (%)	0.62±0.04	1.18±0.11[a]	0.71±0.07[b]	0.97±0.04[a,b]	0.95±0.02[a,b]	0.89±0.04[b]	1.01±0.99[a]

a = Significant increase when compared with the control group (p<.05)
b = Significant increase when compared with the benz[a]anthracene group (p<.05)
B[a]A = Benz[a]anthracene
* Mean ± SEM of 6 observations

The administration of benz[a]anthracene did not result in a significant distinction (p>.05) between the post-induction ALT levels and the pre-induction ALT levels across all treatment groups. However, the post-treatment ALT value (68.90±5.04 U/L) in the benz[a]anthracene group exhibited a significant decrease (p<.05) compared to the post-induction value (83.13±9.07 U/L) observed 21 days after the cessation of induction. The post-treatment ALT levels (67.62±1.12 and 71.70±4.69 U/L) of ETF and HXF treated groups respectively were significantly lower (p<.05) compared with their ALT pre-induction values (100.97±4.29 and 80.23±5.69 U/L respectively). There was however, a significant decrease (p<.05) in the post-treatment ALT value of the HXF-treated group when

compared with the HXF post-induction ALT values (108.02±11.02). The significant decrease (p<.05) in the post-treatment ALT value of the HXF-treated group when compared with the post-induction ALT values (108.02±11.02) was evident. There was no significant difference (p>.05) when post-treatment ALT levels of the treatment groups were compared to that of the control, benz[a]anthracene or diclofenac-treated groups.

The post-induction ALP levels in the serum exhibited a significant increase (p<.05) in all treatment groups, excluding the control group, when compared to their respective pre-induction ALP values. There was no significant difference (p>.05) between the pre-induction (30.75±5.84 IU/L), post-induction (30.65±6.23 IU/L), and, post-treatment (30.40±6.33 IU/L) ALP levels of the control group. The post-treatment ALP levels decreased significantly (p<.05) after 21 days of treatment with the different solvent fractions and diclofenac except with the EAF-treated groups when compared with their respective post-induction ALP values. There was no significant difference when the post-treatment ALP value (33.75±5.15 IU/L) of the EAF-treated group was compared to the post-treatment ALP values (33.05±5.42 IU/L) of the benz[a]anthracene group (Table 4).

The administration of benz[a]anthracene did not elicit any significant response (p>.05) in the serum urea level of the animals. A significant increase (p<.05) in the post-treatment urea levels was observed with the toxicant-only group, EAF, DEF, HXF, and, diclofenac-treated groups (8.68±0.82, 6.54±0.58, 7.90±0.58, 6.84±0.49 and, 9.30±0.58 mmol/L respectively) when compared to their pre-induction urea levels (5.01±0.58, 4.31±0.17, 4.77±0.53, 4.89±0.55 and, 5.12±0.79 mmol/L respectively). The post-treatment serum urea levels of the toxicant-only, DEF, and diclofenac-treated groups were significantly increased (p<.05) when compared to their post-induction urea levels (6.04±0.37, 5.54±0.24 and 5.76±0.53 mmol/L respectively). There was no significant difference (p>.05) between the post-treatment urea level (4.41±0.36 mmol/L) of the ETF-treated group in both the pre-induction (5.51±0.29 mmol/L) and post-induction (5.29±0.32 mmol/L) urea levels (Table 4).

The post-induction serum creatinine levels were significantly increased (p<.05) in most of the treatment groups when compared with their pre-induction creatinine levels (Table 4). The post-treatment creatinine level of the ethanol fraction (69.78±8.03 µmol/L) was significantly increased (p<.05) when compared to the ethanol fraction pre-induction creatinine level (57.05±3.49 µmol/L). There was a significant decrease (p<.05) in the post-treatment creatinine level (56.20±4.42 µmol/L) of the DEF-treated group when compared with the post-induction creatinine level (69.82±4.52 µmol/L). No significant (p>.05) alterations in the pre-treatment creatinine levels of the benz[a]anthracene-only, EAF, HXF, and diclofenac-treated groups were observed when compared with their post-induction creatinine values.

3.4 Effects of Different Solvent Fractions of *Curcuma longa* on the Haematological Indices to Benz[A]Anthracene-induced Toxicity in Rats

After 21 days of the administration, there was no significant impact (p>.05) of benz[a]anthracene on the values of all haematological parameters when compared to their respective pre-induction values across all treatment groups (Table 5).

The post-treatment PCV values of the control (37.36±1.43%), benz[a]anthracene (39.00±0.37%), and ETF (35.5±0.76%) treated groups were significantly increased (p<.05) when compared with their pre-induction values (29.83±2.31, 31.00±0.37 and 33.0±0.73% respectively). The post-treatment PCV values (31.83±1.01, 31.67±3.54 and 32.17±2.70 %) of the EAF, DEF, and diclofenac-treated groups were significantly decreased (p<.05) when compared to the post-treatment PCV values of the benz[a]anthracene group. The post-treatment PCV values (39.00±0.37 and 36.83±1.08%) of the benz[a]anthracene and HXF-treated group were significantly increased (p<.05) when compared with their post-induction PCV values (31.00±0.37 and 28.33±0.92%) respectively.

The treatment with HXF and diclofenac increased significantly (p<.05) the post-induction

RBC count of 4.06±0.38 and 3.83±0.27 x 10^{12}/L respectively to a post-treatment RBC count of 5.09±0.20 and 5.28±0.21 x 10^{12}/L respectively. Although there was no significant difference (p>.05) between the post-induction (4.67±0.35 x 10^{12}/L) and post-treatment (4.67±0.13 x 10^{12}/L) RBC counts of the benz[a]anthracene group, the post-treatment RBC count was significantly lower (p<.05) when compared to the pre-induction RBC count (5.70±0.31 x 10^{12}/L).

There was a significant increase (p<.05) in the post-treatment WBC counts (6.79±0.73 and 5.60±0.90 x 10^{9}/L) of the ETF and diclofenac-treated groups respectively

Table 4. Mean* serum biochemical parameters in Wistar rats treated with *C. longa* methanol extract fractions after benz[a]anthracene exposure

Parameters		Treatment groups						
	Sampling time	Control	Benz[a] anthracene (25mg/kg)	B[a]A + Ethanol fraction (25mg/kg)	B[a]A + Ethyl acetate fraction (25mg/kg)	B[a]A + Diethyl ether fraction (25mg/kg)	B[a]A + *n*-Hexane fraction (25mg/kg)	B[a]A + Diclofenac Na (10mg/kg)
AST	Pre-induction	288.18±30.45	255.72±22.96	275.45±5.62	270.01±5.84	270.82±12.17	275.23±8.39	259.63±5.02
(U/L)	Post-induction	279.15±25.58	330.80±27.22	275.52±22.2	318.05 ±29.43	312.48±8.35	330.33±42.73	292.18±13.43
	Post-treatment	264.05±23.99	313.84±51.84^{a}	168.85±7.45^{a*,b,c}	212.87±15.96^{a*,b}	193.63±8.48^{a*,b,c}	218.85±11.57^{a*}	237.07±24.32
ALT	Pre-induction	95.85±10.44	70.88±4.70	100.97±4.29	79.50±3.52	98.20±22.82	80.23±5.46	88.80±4.83
(U/L)	Post-induction	90.93±13.05	83.13±9.07	92.83±5.83	80.13±3.69	73.42±6.58	108.02±11.02	88.17±9.21
	Post-treatment	91.47±16.19	68.90±5.04^{b}	67.62±6.52	104.65±14.44	80.68±8.13	71.70±4.69^{b}	82.17±4.45
ALP	Pre-induction	30.75±5.84	21.38±1.21	28.57±2.78	23.40±1.67	23.27±1.91	23.81±1.65	33.93±4.06
(IU/L)	Post-induction	30.65±6.23	53.73±4.97^{a}	51.28±1.66^{a}	43.03±5.76^{a}	43.73±0.65^{a}	54.82±7.25^{a}	54.87±3.99^{a}
	Post-treatment	30.40±6.33	33.05±5.42	16.28±1.12^{a*,b,d}	33.75±5.15	26.08±1.90^{b}	28.23±1.68^{b}	25.50±0.82^{b}
UREA	Pre-induction	5.58±0.72	5.01±0.58	5.51±0.29	4.31±0.17	4.77±0.53	4.89±0.55	5.12±0.79
(mmol/L)	Post-induction	5.81±0.76	6.04±0.37	5.29±0.32	6.01±0.13	5.54±0.24	5.56±0.26	5.76±0.53
	Post-treatment	5.69±0.83	8.68±0.82^{a,b*}	4.41±0.36	6.54±0.58^{a}	7.90±0.58^{a,b*}	6.84±0.49^{a}	9.30±0.58^{a,b*}
CREATININE	Pre-induction	61.67±5.88	50.73±1.65	57.05±3.49	58.32±2.59	59.00±3.28	63.83±3.73	55.07±4.13
(µmol/L)	Post-induction	61.18±7.65	68.17±3.96^{a}	63.02±3.34	73.75±4.65^{a}	69.82±4.52^{a}	60.10±2.39	55.47±4.27
	Post-treatment	65.75±6.99	62.75±2.99	73.08±4.52^{a,b*}	64.42±2.78	56.20±4.42^{b}	62.23±2.78	69.78±8.03

a = Significant increase compared with the pre-induction value (p<.05)
b = Significant decrease compared with the post-induction value (p<.05)
c = Significant decrease compared with the toxicant group (p<.05)
d = Significant decrease compared with the diclofenac group (p<.05)
*=Mean ± SEM of 6 observations

a* = Significant decrease compared with the pre-induction value (p<.05)
b* = Significant increase compared with the post-induction value (p<.05)
Key: AST = Aspartate Aminotransferase; ALT = Alanine Transferase; ALP = Alkaline Phosphatase

Table 5. Mean* haematological parameters in Wistar rats treated with *C. longa* methanol extract fractions after benz[a]anthracene exposure

Parameters		Treatment groups						
	Sampling time	Control	B[a]A (25mg/kg)	B[a]A + ETF (25mg/kg)	B[a]A + EAF (25mg/kg)	B[a]A + DEF (25mg/kg)	B[a]A + HXF (25mg/kg)	B[a]A + Diclofenac Na (10mg/kg)
PCV (%)	Pre-induction	27.17±1.22	31.67±1.28	27.5±1.93	29.16±1.19	30.83±1.67	31.83±1.64	31.00±2.03
	Post-induction	29.83±2.31	31.00±0.37	33.0±0.73	30.17±1.35	33.83±0.95	28.33±0.92	32.67±1.12
	Post-treatment	37.36±1.43^{a}	39.00±0.37^{a,b}	35.5±0.76^{a}	31.83±1.01^{c}	31.67±3.54^{c}	36.83±1.08^{b}	32.17±2.70^{c}
RBCs (x 10^{12}/L)	Pre-induction	4.80±0.58	5.70±0.31	4.99±0.54	4.88±0.44	4.82±0.48	6.60±0.63	5.06±0.31
	Post-induction	3.71±0.60	4.67±0.35	4.36±0.38	4.33±0.38	4.40±0.21	4.06±0.38	3.83±0.27
	Post-treatment	5.09±0.23	4.67±0.13^{a*}	4.98±0.33	4.37±0.27	4.99±0.46	5.09±0.20^{b}	5.28±0.21^{b}
WBCs (x 10^{9}/L)	Pre-induction	4.55±0.47	6.80±0.58	3.95±0.53	6.93±1.44	5.13±0.76	5.67±0.97	3.70±0.45
	Post-induction	4.17±0.68	4.20±0.58	6.63±2.19	7.27±0.72	5.75±0.78	6.22±0.68	4.10±0.43
	Post-treatment	7.87±0.72^{a,b}	6.13±0.79	6.79±0.73^{a}	6.23±0.98	6.97±1.01	7.02±0.68	5.60±0.90^{a}
NEUTROPHILS	Pre-induction	35.0±4.02	36.50±4.51	50.0±1.86	44.33±3.41	46.00±2.72	36.83±2.82	45.00±5.34
(%)	Post-induction	36.17±2.44^{c}	56.00±2.85	40.33±6.24	46.17±5.30	41.17±4.59	45.67±4.83	44.00±2.97
	Post-treatment	35.33±3.77	26.33±2.56^{a*,b*}	26.33±4.29^{a*,b*}	33.50±3.32^{a*,b*}	28.67±2.80^{a*,b*}	20.50±2.01^{a*,b*}	24.83±2.06^{a*,b*}
EOSINOPHILS	Pre-induction	0.50±0.34	0.67±0.21	0.00±0.00	0.17±0.17	0.17±0.17	0.33±0.21	0.17±0.17
(%)	Post-induction	1.00±0.45	0.33±0.21	0.33±0.21	1.00±0.37	0.50±0.22	0.50±0.34	0.50±0.22
	Post-treatment	1.00±0.32	0.17±0.17	1.83±0.65	0.50±0.22	0.67±0.33	1.00±0.45	0.50±0.22
BASOPHILS	Pre-induction	0.00±0.00	0.00±0.00	0.00±0.00	0.00±0.00	0.00±0.00	0.00±0.00	0.00±0.00
(%)	Post-induction	0.00±0.00	0.00±0.00	0.00±0.00	0.17±0.17	0.17±0.17	0.00±0.00	0.00±0.00
	Post-treatment	0.00±0.00	0.00±0.00	0.17±0.17	0.00±0.00	0.00±0.00	0.00±0.00	0.00±0.00
LYMPHOCYTES	Pre-induction	58.83±3.91	59.83±4.11	46.83±1.94	50.33±3.38	48.00±2.42	57.83±2.46	49.67±5.31
(%)	Post-induction	56.17±2.18	38.33±2.79	52.83±6.48	48.17±4.83	54.33±4.52	47.50±4.63	51.00±2.78
	Post-treatment	56.67±4.09	67.33±2.38^{a,b}	65.50±4.67^{a,b}	61.33±3.19^{a,b}	64.83±1.64^{a,b}	72.67±1.87^{a,b}	69.33±2.03^{a,b}
MONOCYTES	Pre-induction	5.67±0.61	3.00±0.26	3.17±0.70	5.17±0.48	5.83±0.70	5.00±0.45	5.17±0.60
(%)	Post-induction	6.83±1.01	5.33±0.84	6.50±0.56	4.50±0.67	3.83±0.87	6.33±0.84	4.50±0.62
	Post-treatment	6.80±0.66	6.00±0.37^{a}	6.33±0.56^{a}	4.67±0.88	5.67±0.99^{b}	5.83±0.60	5.17±1.01

a = Significant increase compared with the pre-induction value (p<.05),
b = Significant increase compared with the post-induction value (p<.05),
c = Significant decrease compared with the toxicant treated group (p<.05)

a* = Significant decrease compared with the pre-induction value (p<.05)
b* = Significant decrease compared with the post-induction value (p<.05)
*=Mean ± SEM of 6 observations

compared to their pre-induction WBC counts (3.95±0.53 and 3.70±0.45 x 10^9/L respectively). The post-treatment total WBC count (7.87±0.72 x 10^9/L) of the control group was significantly increased (p<.05) when compared with both the pre and post-induction total WBC count (4.55±0.47 and 4.17±0.68 x 10^9/L respectively).

The post-treatment neutrophils count showed that the benz[a]anthracene group, all the solvent fraction treatment groups, and the diclofenac treatment group were all significantly decreased (p<.05) when compared with both their individual pre and post-induction values respectively. However, the control group showed no significant difference (p>.05) when the post-treatment value (35.33±3.77%) was compared to both the pre and post-induction neutrophils values (35.0±4.02 and 36.17±2.44 % respectively). Conversely, the post-treatment lymphocyte counts showed that the benz[a]anthracene group, all the solvent fraction treatment groups, and the diclofenac treatment group were all significantly increased (p<.05) when compared with both their individual pre and post-induction values respectively. However, the control group showed no significant difference (p>.05) when the post-treatment lymphocyte value (56.67±4.09%) was compared to both the pre and post-induction lymphocyte values (58.83±3.91 and 56.17±2.18 % respectively) (Table 5).

There was a significant increase (p<.05) in the post-treatment monocyte count values (6.00±0.37 and 6.33±0.56%) of the benz[a]anthracene and ETF-treated groups respectively when compared to their pre-induction monocyte count values (3.00±0.26 and 6.33±0.56% respectively). There was no significant difference (p>.05) between the post-treatment and pre or post-induction eosinophils and basophils count values of all the treatment groups (Table 5).

3.5 The Effects of Different Solvent Fractions of *Curcuma longa* on the Serum Levels of Oncogenic Biomarkers to Benz[A]Anthracene-induced Toxicity in Rats.

Exposure to benz[a]anthracene significantly increased (p<.05) the serum levels of EGFR, CA 125, and, CEA in 50, 100, and 50 % respectively of the test population when compared to their pre-induction serum levels. In contrast, benz[a]anthracene did not significantly affect (p<.05) the serum levels of CYFRA 21-1 in comparison with the pre-induction serum CYFRA 21-1 levels (Table 6).

The post-treatment serum levels of EGFR and CYFRA 21-1 were significantly decreased (p<.05) when compared to their post-induction values in all the treatment groups (Table 6). Nevertheless, when compared across the columns, the post-treatment serum EGFR levels of the HXF (20.85±0.90 ng/L) treated group were significantly lower (p<.05) compared to the post-treatment serum EGFR levels (21.92±1.15 ng/L) of the benz[a]anthracene group. Likewise, the post-treatment serum CYFRA 21-1 levels (13.98±1.67 ng/L) of the DEF-treated group were significantly lower (p<.05) compared to the post-treatment serum CYFRA 21-1 levels (15.60±1.65 ng/L) of the benz[a]anthracene treated group as represented in Table 6.

The post-treatment serum CA 125 levels were significantly increased (p<.05) in all the treatment groups when compared to their pre-induction serum CA 125 levels; except the serum CA 125 levels (0.91±0.15 U/mL) of the EAF-treated group was rather significantly decreased (p<.05) compared with the post-induction serum CA 125 levels (1.14±0.41 U/mL). The post-treatment serum CA 125 levels (0.91±0.15, 1.87±0.34, 1.68±0.63 and 2.60±0.56 U/mL) of EAF, DEF, HXF, and diclofenac treated groups respectively were significantly decreased (p<.05) compare to the post-treatment serum CA 125 levels (5.41±2.65 U/mL) of the benz[a]anthracene treated groups. Conversely, the treatment with ETF, EAF, and diclofenac significantly decreased (p<.05) the serum CEA levels from their post-induction values of 5.92±0.27, 6.13±0.39 and 6.08±0.28 ng/mL respectively to the post-treatment values of 4.92±0.56, 5.25±0.30, and 5.41±2.65 ng/mL respectively. Nevertheless, the post-treatment serum CEA levels (7.49±0.38 and 5.01±0.29 ng/mL) of the benz[a]anthracene and HXF-treated groups respectively were significantly higher (p<.05) than the pre-induction CEA levels (4.86±0.13 and 4.64±0.27 ng/mL respectively), 21 days after the induction was discontinued. The post-treatment serum CEA levels of all the treatment groups were significantly decreased (p<.05) compared to the post-treatment serum CEA values of the benz[a]anthracene group (Table 6).

3.6 Effect of the Different Solvent Fractions of *Curcuma longa* on Tissue Biochemical Parameters

The lung tissue biochemical activity of rats exposed to benz[a]anthracene and treated with different solvent fractions of *C. longa* are shown in Table 7. The GST

Table 6. Mean* serum concentration of oncogenic biomarkers in Wistar rats treated with *C. longa* methanol extract fractions after benz[a]anthracene exposure

Treatment groups							
Parameter	**Sampling time**	**Benz[a] anthracene (25 mg/kg)**	**Benz[a] anthracene + Ethanol fraction (25 mg/kg)**	**Benz[a] anthracene + Ethylacetate fraction (25 mg/kg)**	**Benz[a] anthracene + Diethyl ether fraction(25 mg/kg)**	**Benz[a] anthracene + *n*-Hexane fraction(25 mg/kg)**	**Benz[a] anthracene + Diclofenac Na (10 mg/kg)**
EGFR (ng/L)	Pre-induction	27.83±2.02	37.56±2.61	44.94±3.50	36.34±2.61	39.97±2.53	37.58±3.16
	Post-induction	41.21±1.26[a]	35.31±2.60	40.32±0.64	45.95±0.61[a]	39.16±0.19	45.74±1.31[a]
	Post-treatment	21.92±1.15[b]	22.92±1.31[b]	22.54±1.17[b]	25.90±1.24[b]	20.85±0.90[b,c]	28.10±2.60[b]
CYFRA 21-1 (ng/L)	Pre-induction	18.14±0.21	16.55±0.07	17.65±0.17	16.87±0.18	15.23±0.58	15.91±0.39
	Post-induction	17.01±1.39	15.20±0.44	15.20±0.11	14.77±0.11	15.55±0.19	15.50±0.48
	Post-treatment	15.60±1.65[b]	14.96±1.74[b]	14.29±0.69[b]	13.98±1.67[b,c]	14.33±1.83[b]	14.80±1.70[b]
CA 125 (U/mL)	Pre-induction	0.55±0.05	0.43±0.10	0.42±0.02	0.41±0.14	0.35±0.04	0.53±1.05
	Post-induction	1.22±0.34[a]	1.18±0.20[a]	1.14±0.41[a]	0.95±0.25[a]	0.60±0.22[a]	1.33±0.29[a]
	Post-treatment	5.41±2.65[a]	9.86±5.47[a]	0.91±0.15[b,c]	1.87±0.34[a,c]	1.68±0.63[a,c]	2.60±0.56[a,c]
CEA (ng/mL)	Pre-induction	4.86±0.13	4.92±0.25	4.94±0.07	5.24±0.08	4.64±0.27	4.58±0.19
	Post-induction	5.08±0.11	5.92±0.27[a]	6.13±0.39[a]	5.51±0.27	4.79±0.07	6.08±0.28[a]
	Post-treatment	7.49±0.38[a]	4.92±0.56[b,c]	5.25±0.30[b,c]	5.22±0.26[c]	5.01±0.29[a,c]	5.41±2.65[b,c]

a = Significant increase compared with the pre-induction value (p<.05)
b = Significant decrease with the post-induction value (p<.05)
c = Significant decrease with the toxicant group (p<.05)
*=Mean ± SEM of 6 observations

Key:
EGFR = Epidermal Growth Factor Receptor
CYFRA 21-1 = Cytokeratin Fragment Antigen 21-1
CA 125 = Cancer Antigen 125

activity of the benz[a]anthracene (29.55±14.39 U/mg protein) and diclofenac-treated (157.00±45.37 U/mg protein) groups were significantly decreased (p<.05) when compared with the control (231.22±13.95 U/mg protein). The treatment groups; ethanol fraction, ethyl acetate fraction, diethyl ether fraction, *n*-hexane fraction, and diclofenac were statistically similar. However, the GST activities of ETF (200.03±56.83) and EAF (192.46±58.34) treated groups were statistically similar to the control group.

The GPx activities of the lung tissue of the control group (26.17±3.58 U/mg protein) and those of the different treatment groups including that of the ETF (23.73±4.80 U/mg protein) and DEF (23.79±5.05 U/mg protein) were statistically similar. The GPx activity of toxicant (17.69±1.71 U/mg protein), HXF (16.05±3.71 U/mg protein), and diclofenac (17.49±2.61 U/mg protein) treated groups were statistically similar and significantly decreased (p<.05) compared to the control. The GPx activity (34.09±4.70 U/mg protein) of the EAF-treated group was significantly increased compared to the control group.

The GR activity of the benz[a]anthracene alone treated group (240.55±83.82 U/mg protein) was significantly increased (p<.05) compared to the control (46.06±25.47 U/mg protein). The GR activities of the control (46.06±25.47 U/mg protein), ethanol fraction (58.29±17.50 U/mg protein), ethyl acetate fraction (42.50±11.72 U/mg protein), and *n*-hexane fraction (21.58±9.29 U/mg protein) treatment groups were significantly decreased (p<.05) when compared to the benz[a]anthracene alone treated group. There were no significant differences (p>.05) between the GSH activities (101.62±22.96 and 114.82±16.54 U/mg protein) of the control and the EAF-treated group respectively. The GSH activities (38.88±8.61, 71.48±11.08, 72.07±12.59, 58.28±10.72, and 35.22±8.21 U/mg protein) of the toxicant, ETF, DEF, HXF and diclofenac-treated groups respectively were significantly lower (p<.05) than the GSH activity of the control group whilst the toxicant group was statistically similar to the diclofenac treated group. The toxicant (14.47±3.04 U/mg protein), HXF (16.72±4.23 U/mg protein), and diclofenac (19.55±3.51 U/mg

protein) treated groups were statistically similar but significantly decreased ($p<.05$) compared to the control (26.87±4.07 U/mg protein) group, concerning the SOD activities. There was no significant difference between the SOD activities (26.87±4.07 and 24.14±4.48 U/mg protein) of the control and DEF-treated groups respectively, however, the SOD activity (32.16±4.70 U/mg protein) of the EAF-treated group was significantly higher ($p<.05$) than the control group (Table 7).

3.7 Histopathological Findings in Rats Exposed Benz[a]anthracene and Treated with Solvent Fractions of *Curcuma longa* Extract

3.7.1 Histopathological Picture of Lung Tissue of Control Rat

Figure 1 shows the respiratory tissue of the control rat. The alveoli sacs at the TOP LEFT are normally outlined. At the TOP RIGHT and LOWER RIGHT, the muscular wall of the bronchiole and respiratory bronchiole were mildly infiltrated with inflammatory cells. There are congested vascular channels with thickened muscular walls at the LOWER LEFT. The tissue injury score is 5.56% as represented in Table 8.

3.7.2 Histopathological Picture of Post-induction Lung Tissue (Day 21)

The alveoli wall is thickened and constricted with a slight hemorrhage at the top left quadrant of Figure 2, degenerating Congested Vessels (CV) are also seen. The muscular wall of the bronchioles (B) at the top right is thickened and infiltrated with inflammatory cells having reactive nuclei. The adjacent CV is also infiltrated by inflammatory cells. The lower left quadrant reveals a distorted congested vessel with red blood cells (thick arrow). Its wall is thickened and an adjacent granulation reaction seedling (thin arrow) is seen. At the lower right, however, constricted vessels and constricted Alveoli Sacs (AT) are seen. The bronchiole (B) is infiltrated by inflammatory cells and areas with interstitial haemorrhage are seen. The tissue injury score of the post-induction lung tissue (TOX I) is 45.45% which is significantly increased ($p<.05$) compared to the tissue injury score (5.56%) of the control group as represented in Table (8). These overall features are in keeping with moderate to severe pneumonitis.

3.7.3 Histopathological Picture of Lung Tissue Section of Untreated Rats (Day 42)

The TOP LEFT quadrant of Figure 3 shows proliferating bronchioles (B) with distorted architecture. The cells

Table 7. Mean* Lung tissue antioxidant activities in Wistar rats treated with *C. longa* methanol extract fractions after benz[a]anthracene exposure

Treatment groups		Antioxidant activities			
	GST(U/mg protein)	GP_x(U/mg protein)	GR(U/mg protein)	GSH(U/mg protein)	SOD (U/mg protein)
Control	231.22±13.95	26.17±3.58	46.06±25.4^{7b}c	101.62±22.96	26.87±4.07
Benz[a]anthracene (25mg/kg)	29.55±14.39^{a}	17.69±1.7^{1a,}b	240.55±83.8^{2a*}	38.88±8.6^{1a,}b	14.47±3.0^{4a,}b
Benz[a]anthracene + Ethanol fraction (25mg/kg)	200.03±56.83^{d}	23.73±4.80^{d}	58.29±17.50^{b,c}	71.48±11.08^{a}	21.74±3.50^{b}
Benz[a]anthracene + Ethyl acetate fraction (25mg/kg)	192.46±58.3^{4}d	34.09±4.7^{0a*}	42.50±11.^{72b},c	114.82±16.5^{4}d	32.16±4.70^{a*}
Benz[a]anthracene + Diethyl ether fraction (25mg/kg)	141.11±41.8^{6}b	23.79±5.0^{5}d	104.18±71.8^{6a*,}c	72.07±12.5^{9}a	24.14±4.48^{d}
Benz[a]anthracene + *n*-Hexane fraction (25mg/kg)	81.46±51.1^{3}b	16.05±3.7^{1a,}b	21.58±9.2^{9a,}c	58.28±10.7^{2}a	16.72±4.23^{a,b}
Benz[a]anthracene + Diclofenac Na (10mg/kg)	157.00±45.3^{7}a	17.49±2.6^{1}a	51.89±9.6$^{8\ c,}$d	35.22±8.2^{1}a	19.55±3.51^{a}

a = Significant decrease compared to control animals ($p<.05$);
b = No significant difference from the diclofenac-treated group ($p>.05$)
c = Significant decrease compared to the toxicant group ($p<.05$)
d = No significant difference from the control group ($p>.05$)

a* = Significant increase compared to control animals ($p<.05$)
*Mean ± SEM of 6 observations,

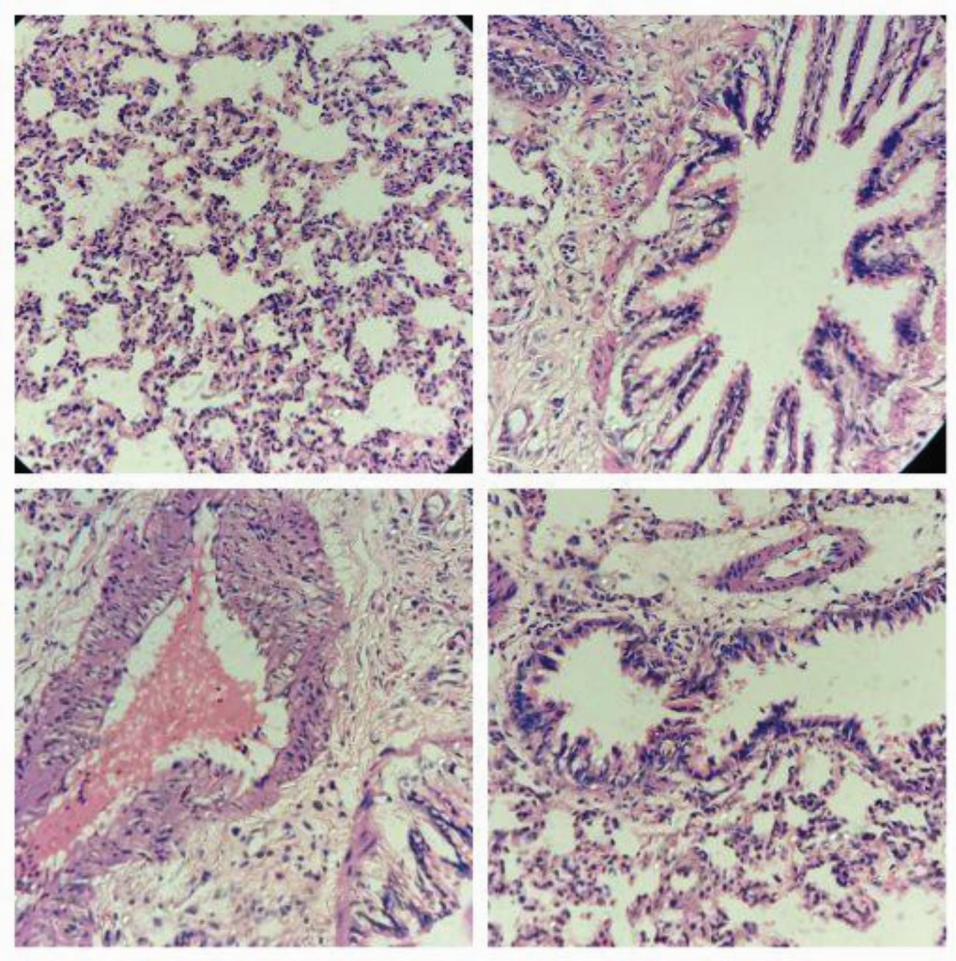


Figure 1. Histopathology sections of lung tissue architecture of a rat treated with only water as negative control
Section of the lung tissue show apparently normal lung tissue architecture outlines

of the epithelial lining have enlarged nuclei. The adjacent vessel is also congested and distorted. Marked haemorrhage within the tissue body is seen at the TOP RIGHT quadrant of Figure 3; beside which is seen a vessel (BV) with a thickened vascular wall, partially dilated and congested, and its lumen containing eosinophilic material admixed with scanty inflammatory deposits. The lower left, however, shows distorted and infiltrating bronchioles (B) and dilated vessels (BV) filled with red blood cells in its lumen. However, at the lower right, the alveoli sacs (CA) are congested and dilated, and hence the architecture is distorted. The alveoli wall is thickened, lymphocyte aggregated (IF), and the alveoli are haemorrhaged (H). Congested and constricted vessels (thin arrow) are also seen. The tissue injury score of the untreated group (TOX II) is 75% which is more than the tissue injury score (45.45%) of the TOX I. It is significantly increased ($p<.05$) compared to the tissue injury score (5.56%) of the control group as represented in Table 8. These overall features are in keeping with severe pneumonitis.

3.7.4 Histopathology Picture of the Lung Tissue of a Rat Treated with Ethanol Fraction of Curcuma longa Rhizome

The bronchioles (B) are reactive, constricted, and infiltrated by inflammatory cells consequently distorting the muscular wall as seen on the top left and top right of Figure 4. The Alveolar Wall (AW) is infiltrated and granulated by inflammatory cells, hence the walls are thickened and the alveoli sacs collapse (AT). Vessels (CV) are constricted, the lumen is congested with eosinophilic material admixed with inflammatory cells, and the walls are infiltrated by inflammatory cells (IF) hence, thickened, degenerative, and distorted (lower left and right of Figure 4). At the lower left also is seen

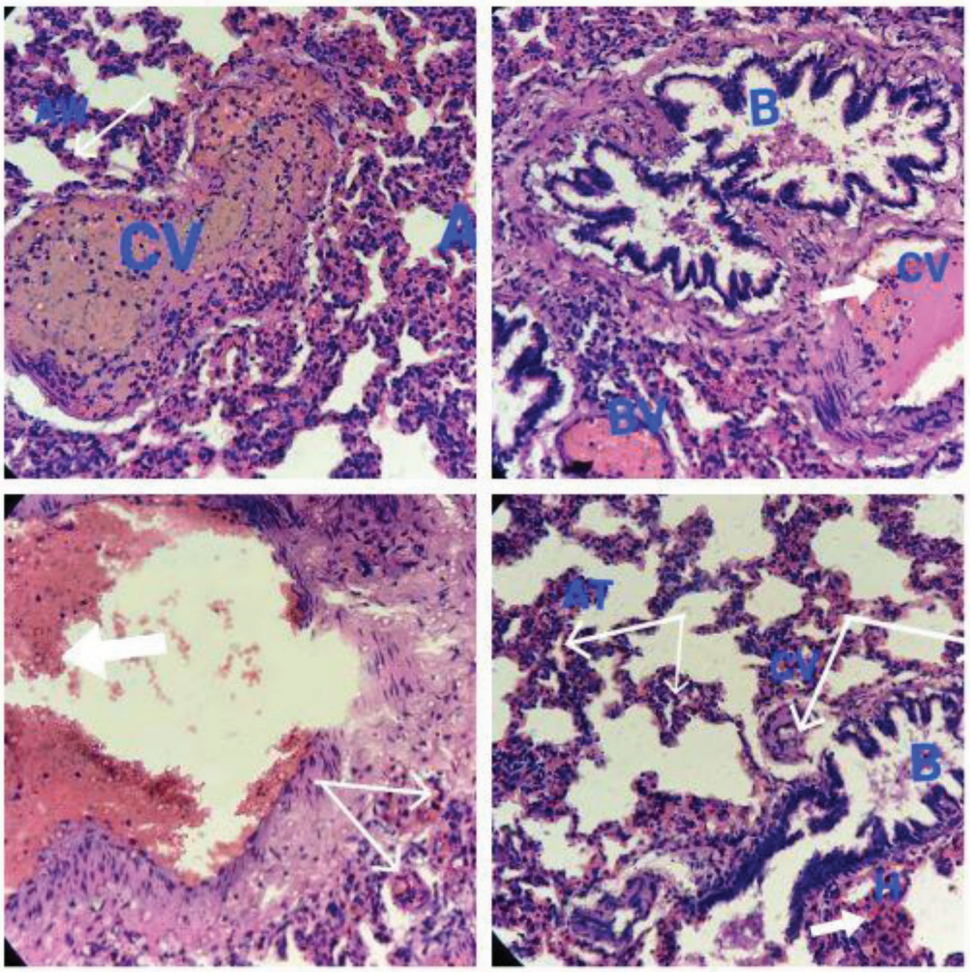


Figure 2. Histopathology sections of lung tissue architecture of a rat treated with benz[a]anthracene for 21 days designated TOX I. Sections showing Congested Vessel (CV), thickened Alveoli Wall (AW), alveoli wall haemorrhage (A), bronchioles (B), Congested Vessel (CV), distorted vessel congested with red blood cells (thick arrow – lower left) with thickened wall showing adjacent granulation reaction seedlings (thin arrow – lower left), collapsed alveoli sacs (AT), and interstitial haemorrhage (H).

severe inflammatory cell infiltrates (IF) which activate granulation changes. The tissue injury score of the ETF-treated group is 88.63% which is not significantly different ($p>.05$) compared to the tissue injury score (75%) of the TOX II (untreated) group as represented in Table 8. These overall features are in keeping with severe pneumonitis.

3.7.5 Histopathology Picture of the Lung Tissue of Rat Treated with Ethyl Acetate Fraction of Curcuma longa

Figure 5 shows an infiltrated bronchiole (B) with marked aggregates of lymphoid cells infiltrate (IF) (top left) and a distorted bronchiole (B) infiltrated with inflammatory cells admixed with eosinophilic material in its lumen (lower left). At the top and lower right are seen vessels (CV) that are congested, constricted, degenerating, hyalinizing, or dilated with a few having scanty red blood cells in their lumen while some are empty. The alveoli at this point are distorted, and the walls (AW) are infiltrated with inflammatory cells (IF), consequently thickened and granulated. The alveoli sacs (CA) however are congested and variably dilated with background inflammations. The tissue injury score of the EAF-treated group is 37.50% which is significantly decreased ($p<.05$) when compared to the tissue injury score (75%) of the TOX II (untreated) group as represented in Table 8. These overall features are in keeping with mild pneumonitis.

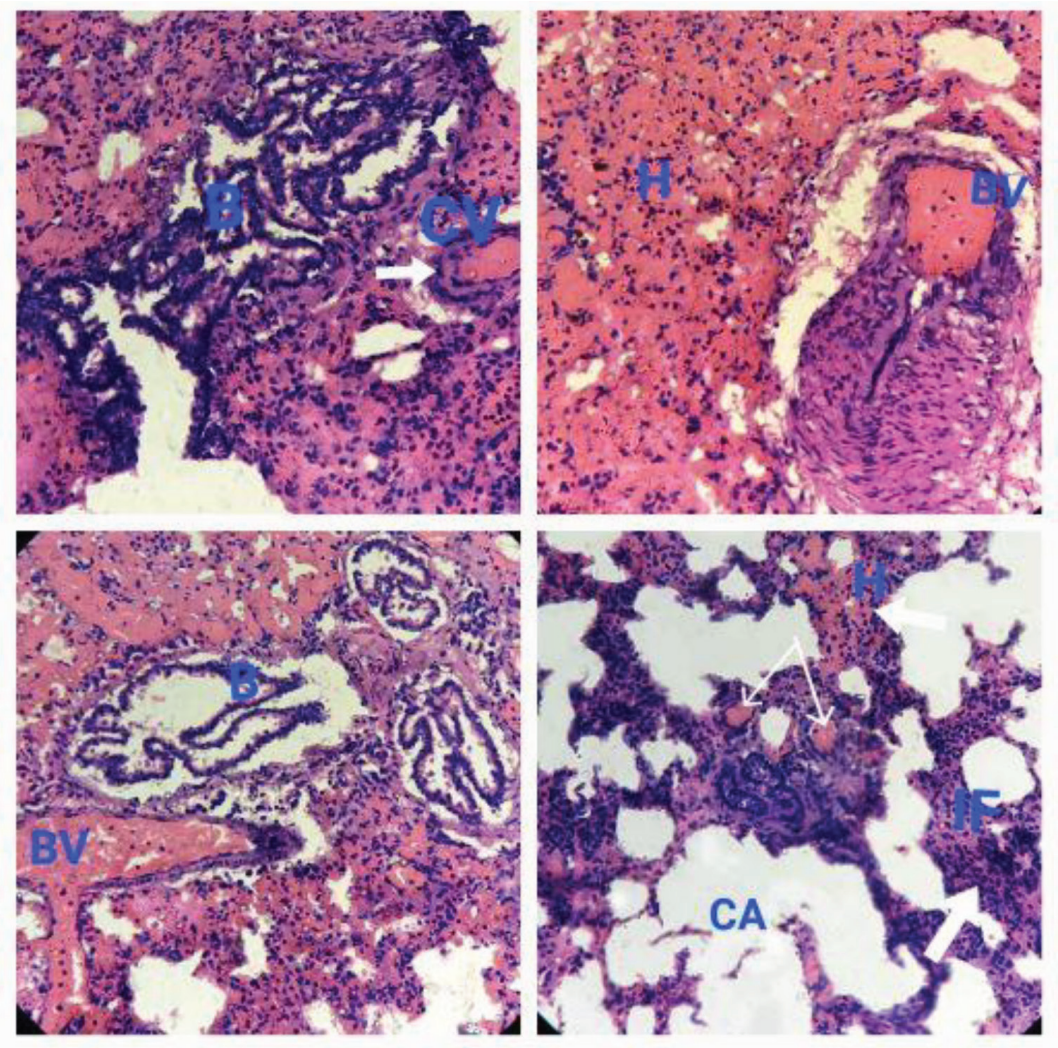


Figure 3. Histopathology sections of lung tissue architecture of a rat treated with benz[a]anthracene for 21 days and left untreated after another 21 days designated TOX II.
Sections showing Bronchioles (B), distorted vessels (CV), shows marked haemorrhage (H), thickened vascular wall (BV), congested alveoli sacs (CA), and aggregate of lymphocytes (IF).

3.7.6 Histopathology Picture of the Lung Tissue of Rat Treated with Diethyl Ether Fraction of Curcuma longa

A markedly dilated, constricted, and congested Blood Vessel (BV) containing red blood cells admixed with eosinophilic material is seen (top and lower left quadrant of Figure 6). There is a severe inflammatory cell (IF) aggregated within the tissue body admix with extravasation red blood cells (H), consequently inducing tissue granulation (top right). The Alveoli Walls (AW) are variably thick and the sacs are Haemorrhaged (H). The lower right quadrant shows moderately infiltrated bronchiole (B) by inflammatory cells that invade and destroy its muscular wall. The tissue injury score of the DEF-treated group is 81.82% which is not significantly different (p>.05) compared to the tissue injury score (75%) of the TOX II (untreated) group as represented in Table 8. The overall features are in keeping with severe pneumonitis.

3.7.7 Histopathology Picture of the Lung Tissue of Rat Treated with Hexane Fraction of Curcuma longa

The histologic features of Figure 7 reveal distorted and dilated bronchiole (B) with reactive hyperchromatic

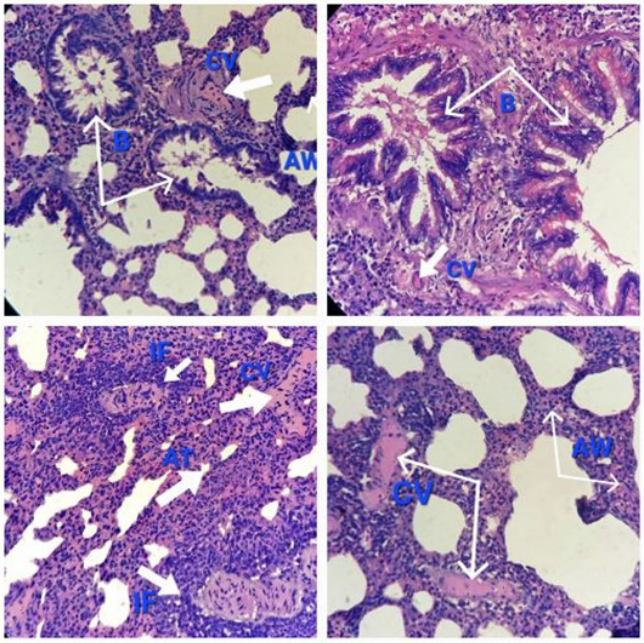


Figure 4. Histopathology sections of lung tissue architecture of a rat treated with ethanol fraction of methanol extract of *Curcuma longa* rhizome in Benz[a]anthracene induced pulmonary toxicity
Sections showing constricted bronchioles (B), Constricted Vessel (CV), thickened alveolar wall (AW), Inflammatory cells infiltrates (IF), Collapsed alveoli sac (AT).

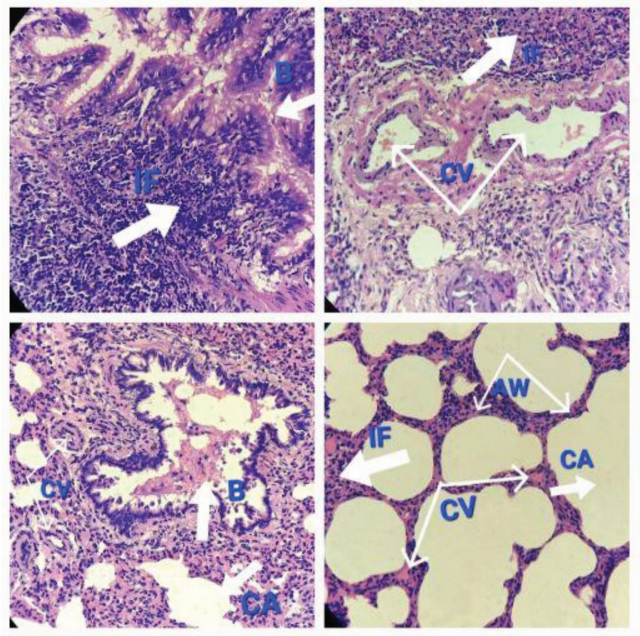


Figure 5. Histopathology sections of lung tissue architecture of a rat treated with ethyl acetate fraction of methanol extract of *Curcuma longa* rhizome in Benz[a] anthracene induced pulmonary toxicity.
Sections showing distorted bronchiole (B), Inflammatory lymphoid aggregate (IF), vessels (CV) congested alveolar sac (CA), and thickened alveoli wall (AW)

nuclei and increased suprabasal eosinophilic material. The muscular wall is disorganized and infiltrated by inflammatory cells. The vascular channel (CV) is congested with eosinophilic material admixed with few inflammatory cells as well as inflammatory cells infiltrated and degenerating Blood Vessels (BV) are seen. The alveolar sac (CA) is dilated and variably congested, while an extended marked congested is seen (top left). The Alveoli Wall (AW) is also variably thickened. The tissue injury score of the HXF-treated group is 56.82% and is significantly decreased compared to the tissue injury score (75%) of the TOX II (untreated) group as represented in Table 8. These features are in keeping with mild pneumonitis.

3.7.8 Histopathological Picture of the Lung Tissue of a Rat Treated with Diclofenac Na

The bronchioles (B) are dilated with a distorted epithelial lining revealing bare floating nuclei with eosinophilic suprabasal material (Figure 8). The vascular channels (CV) are constricted and congested, the lumen is infiltrated by inflammatory cells, and an increase in

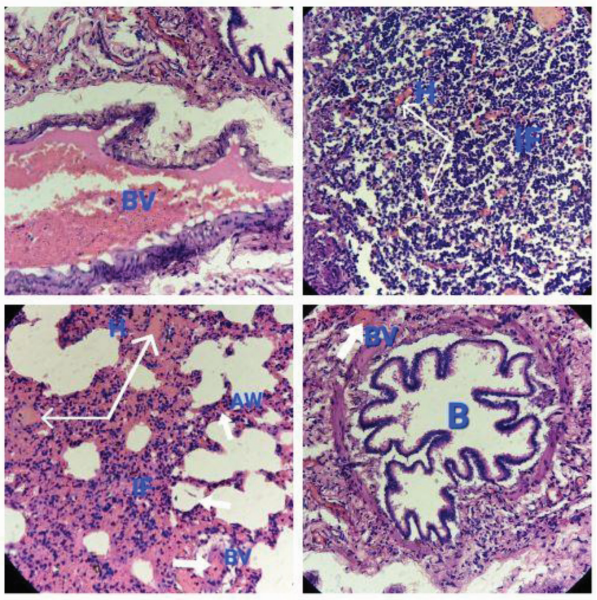


Figure 6. Histopathology sections of lung tissue architecture of a rat treated with diethylether fraction of methanol extract of *Curcuma longa* rhizome in Benz[a] anthracene induced pulmonary toxicity.
Sections showing congested Blood Vessel (BV), inflammatory cells aggregate (IF), Haemorrhage (H), thickened Alveoli Wall (AW), and Bronchiole (B).

Table 8. Lung injury score in Wistar rats treated with *C. longa* methanol extract fractions after benz[a]anthracene exposure

Treatment groups	Median* injury score of lung tissue (percentage damage)								
	Alveolar wall thickness (0 – 16)	Alveolar architecture (0 – 4)	Degree of Cellular infiltration into vascular channels (0 – 4)	Degree of Cellular infiltration into alveolar lumen (0 – 4)	Degree of blood Vessel congestion (0 – 4)	Presence of inflammatory cells (0 – 4)	Overall impression of tissue-level injury (0 – 4)	Hemorrhage (0 – 4)	Total score
Control	0(0)	0(0)	0(0)	0(0)	1(25)	1(25)	0(0)	0(0)	2(5.56)
Benz[a]anthracene (post-induction) (25mg/kg)	4(25)	1(25)	2(50)	4(100)	4(100)	2(50)	1(25)	2(50)	20(45.45)[a]
Benz[a]anthracene (post-treatment) (25mg/kg)	8(50)	2(50)	3(75)	2(50)	3(75)	3(75)	4(100)	4(100)	29(75.00)
Benz[a]anthracene + Ethanol fraction (25mg/kg)	16(100)	3(75)	3.5(87.5)	3.5(87.5)	3.5(87.5)	3.5(87.5)	2.5(62.5)	3.5(87.5)	39(88.63)
Benz[a]anthracene + Ethyl acetate fraction (25mg/kg)	6(37.5)	2.5(62.5)	0(0)	1(25)	1(25)	3(75)	1(25)	2(50)	16.5(37.50)[b]
Benz[a]anthracene + Diethyl ether fraction (25mg/kg)	14(87.5)	4(100)	2(50)	3(75)	3(75)	3(75)	4(100)	3(75)	36(81.82)
Benz[a]anthracene + *n*-Hexane fraction (25mg/kg)	8(50)	3(75)	2(50)	3(75)	3(75)	2(50)	1.5(37.5)	2.5(62.5)	25(56.82)[b]
Benz[a]anthracene + Diclofenac Na(10mg/kg)	6(37.5)	0.5(12.5)	1(25)	2(50)	2.5(62.5)	1.5(37.5)	0.5(12.5)	1.5(37.5)	15.5(35.23)[b]

Keys: 1 = 25%, 2 = 50%, 3 = 75%, 4 = 100%
a = Significant increase ($p < .05$) when compared with the control group
b = Significant decrease ($p < .05$) when compared with Benz[a]anthracene (post-treatment) score
* The median of 6 observations

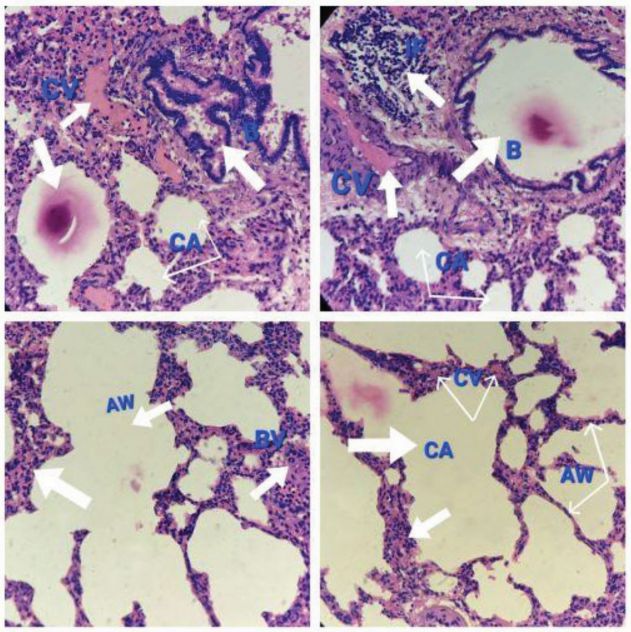


Figure 7. Histopathology sections of lung tissue architecture of a rat treated with n-hexane fraction of methanol extract of *Curcuma longa* rhizome in Benz[a] anthracene induced pulmonary toxicity.
Sections showing distorted Bronchiole (B), Congested Alveolar sacs (CA), marked extension of the congested alveolar sac (Thick arrow – Top left), lymphoid aggregates (IF), Congested Vessel (CV), thickened Alveoli Wall (AW), and degenerating Blood Vessel (BV).

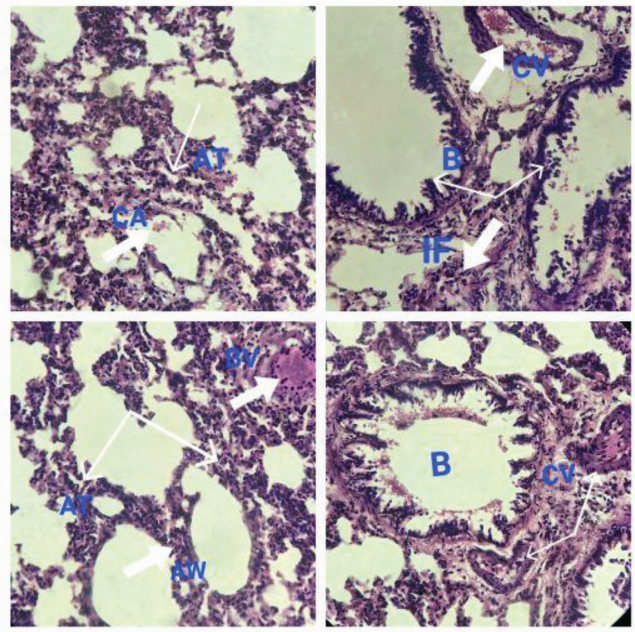


Figure 8. Histopathology sections of lung tissue architecture of a rat treated with Diclofenac Na as a positive control in Benz[a]anthracene induced pulmonary toxicity.
Sections showing Bronchiole (B), Vascular Channels (CV), degenerated vessel (BV), Collapsed alveoli sacs (AT), alveoli wall (AW) with embedded mild inflammatory cells, inflammatory cells infiltrates (IF), and Congested Alveoli sacs (CA).

inflammatory cell infiltrates (IF) is seen within the tissue body. As seen in the lower left; vessel degeneration (BV), collapsed alveoli sacs (AT), dilated alveoli sacs, and relatively normal Alveoli Wall (AW) architecture but the wall is embedded with mild inflammatory cells. The tissue injury score of the diclofenac-treated group is 35.23% which is significantly decreased ($p<.05$) compared to the tissue injury score (75%) of the TOX II (untreated) group as represented in Table 8. These features are in keeping relatively normal respiratory tissue associated with vascular degeneration.

4. Discussion

The yield of the fractions obtained from the partial purification process varied, with the Ethyl Acetate Fraction (EAF showing the highest yield. This was followed by the *n*-Hexane Fraction (HXF), Diethyl Ether Fraction (DEF), and Ethanol Fraction (ETF) with the lowest yield. These variations can be attributed to differences in solvent polarity, solubility of bioactive compounds in the solvents, and extraction efficiency of *C. longa* rhizome[38-40].

The higher yield of the EAF suggests greater solubility of compounds in ethyl acetate compared to ethanol, consistent with previous studies by Arawande *et al.* and Cui *et al.*[41,42] However, some findings contrast with this, where the ethanol fraction yielded more than ethyl acetate fraction[43]. Discrepancies in yields could stem from variations in plant material, purification methods, solvents, or purification conditions[44,45].

The fraction with the highest yield (EAF) may warrant further investigation for its bioactive potential. It could be considered for traditional medicine or pharmaceutical applications[46,47].

Throughout the 21-day exposure to benz[a] anthracene, rats showed a progressive increase in body weight. The group treated solely with benz[a]anthracene exhibited the lowest body weight gain. However, administration of the EAF resulted in the most significant increase in body weight gain among the treated groups.

Benz[a]anthracene is known to induce depression and loss of appetite which potentially explains the

decreased weight gain observed in the benz[a]anthracene group and other treatment groups before solvent fraction administration[48,49]. This aligns with previous findings suggesting weight changes as a symptom of toxicity or adverse health effects[50,51].

The significant increase in body weight gain with the solvent fractions of *C. longa* rhizome methanol extracts suggests their potential ameliorative effects against benz[a]anthracene toxicity. This is likely attributed to the bioactive compounds present in the extracts[52].

In the study, lung-to-body weight ratios significantly increased in groups treated only with the toxicant, EAF, DEF, and diclofenac compared to the control group. However, all solvent fraction-treated groups showed a significant decrease in lung-to-body weight ratios compared to the toxicant-only group. This suggests that while benz[a] anthracene exposure slows weight gain, it also induces pulmonary changes, leading to increased lung size possibly due to inflammation[53]. This aligns with Elshama *et al.* who suggested that changes in lung-to-body weight ratios can be indicative of changes in normal pulmonary cells, with corresponding histopathological abnormalities[54]. Ranieri *et al.* also proposed that increased lung weight could result from acute inflammatory lung injury[55].

The study found that post-induction serum levels of AST and ALT in the benz[a]anthracene-exposed groups did not significantly change compared to their pre-induction levels, suggesting no immediate alterations in liver enzymes. However, post-treatment AST levels significantly decreased in the groups treated with ETF, EAF, and DEF fractions, indicating a potential hepatoprotective effect against benz[a]anthracene-induced changes. AST is predominantly found in hepatocytes and muscle, released during inflammation or injury[56]. The decrease in AST levels may suggest the anti-inflammatory effects of ETF and DEF on liver injury or muscle recovery[57,58]. Importantly, there were no significant differences in post-treatment ALT levels among the treatment groups, suggesting specificity in modulating AST levels and emphasizing the need for further investigation into their mechanisms. These values however are within the normal AST and ALT range for male Wistar rats[59].

The significant increase in ALP levels following benz[a]anthracene induction suggests a general impact on alkaline phosphatase activity, possibly indicating liver or bone involvement[60]. However, post-treatment ALP levels significantly decreased in groups treated with different solvent fractions and diclofenac, except for the EAF-treated group, indicating a potential limitation in mitigating ALP elevation.

The low levels of the post-treatment liver enzymes suggest an improvement in liver health. The disproportionate increase in ALP when compared to ALT and AST levels indicates cholestatic involvement[61], distinguishing it as a characteristic pattern of benz[a] anthracene injury concerning liver function.

The study found that benz[a]anthracene exposure did not significantly affect serum urea levels. However, there was a significant increase in post-treatment urea levels in the toxicant-only group and all the treatment groups except the ETF-treated group. This indicates delayed effects possibly due to stress response or systemic responses beyond direct urea metabolism[62,63]. Some treatment groups experienced a significant increase in post-induction creatinine levels, suggesting benz[a] anthracene's impact on kidney function. Notably, the EAF exacerbated renal damage, while the DEF showed a potential recovery effect on kidney function[63]. Changes in serum urea and creatinine levels are commonly associated with kidney injury, reflecting disruptions in normal filtration and excretion processes[64,65].

Haematological parameters remained largely unaffected by benz[a]anthracene administration. Subsequent treatment resulted in varied effects within the normal range for male Wistar rats[59]. The significant increase in the total white blood cell counts in the ETF-treated group suggests an enhanced immune response, possibly influencing immune cell production or activity. Additionally, benz[a]anthracene and treatment groups exhibited alterations in neutrophil and lymphocyte counts, indicative of immune function changes in response to toxicity[66-68].

The study found significant elevations in EGFR, CA 125, and CEA levels in response to benz[a]anthracene exposure, indicating potential effects on tissues or organs where these biomarkers are primarily expressed[69-72]. Conversely, serum CYFRA 21-1 levels remained unaffected by benz[a]anthracene exposure, suggesting a lack of influence on the pathway regulating CYFRA 21-1 expression[73-75], or suboptimal timing for detecting changes. In the post-treatment, levels of CYFRA 21-1 and EGFR decreased across all groups, indicating a body response to restore physiological balance following cessation of benz[a] anthracene exposure[76,77]. While post-treatment CA 125 levels increased significantly, treatment with EAF, DEF, HXF, and diclofenac mitigated this elevation, potentially

by reducing oxidative stress and inflammation[68,78-80]. By reducing oxidative stress and inflammation, these treatments indirectly lowered CA 125 levels, with EAF treatment showing greater efficacy in mitigation compared to DEF, HXF, and diclofenac treatments.

Serum CEA levels decreased significantly following treatment with ETF, EAF, and diclofenac. The mechanisms underlying the modulation of CEA levels involve complex biological interactions, including inflammation regulation[81-85], detoxification pathways[86,87], or cellular signalling pathways[84,88,89]. Hence the treatment with ETF, EAF, and diclofenac could have interacted with any of these complex biological systems.

The GST activity decreased significantly in the benz[a] anthracene, diclofenac Na, DEF, and HXF-treated groups compared to the control group, indicating potential inhibition by benz[a]anthracene[90-92]. However, the ETF and EAF-treated groups showed GST activities similar to the control group, suggesting a protective effect against benz[a]anthracene-induced decrease[12,93,94]. GPx, GSH, and SOD activities decreased significantly in the benz[a] anthracene, HXF, and diclofenac-treated groups compared to the control group, indicating potential inhibition of antioxidant enzymes by benz[a]anthracene[95-99]. Conversely, the EAF-treated group showed significantly increased GPx, GSH, and SOD activities compared to the control group, suggesting protection against benz[a] anthracene-induced decrease[43,100,101].

GR activity increased significantly in the benz[a] anthracene-treated group compared to the control group, possibly as a compensatory response to oxidative imbalance. However, all treatment groups showed decreased GR activity compared to the benz[a] anthracene-treated group, with the EAF-treated group exhibiting activity similar to the control group. This suggests varying effectiveness in restoring GR activity to normal levels with different solvent fractions[102,103].

Histopathological examination of lung tissue reveals the protective effects of *C. longa* fractions against benz[a] anthracene-induced pneumonitis. Benz[a]anthracene exposure resulted in moderate to severe pneumonitis, indicating significant inflammatory changes in the lung parenchyma. However, treatment with *C. longa* fractions, especially the EAF, showed an improvement in lung histopathology compared to benz[a]anthracene-treated rats alone. The EAF exhibited the most significant reduction in lung tissue injury, suggesting a potential protective effect against pneumonitis.

This improvement in lung histopathology with EAF may indicate its anti-inflammatory properties, which could mitigate the inflammatory response induced by benz[a] anthracene and promote tissue repair and regeneration. The ameliorative effects of EAF on lung histopathology may result from its multifaceted action, including anti-inflammatory and antioxidant properties, along with the quantity and quality of bioactive constituents present in the fraction. Additionally, the pharmacodynamics and pharmacokinetics of the fraction likely contribute to its efficacy.

Furthermore, the fate of bioactive compounds in the living system, determined by factors like bioaccessibility, bioavailability, and bioactivity, plays a crucial role in their effectiveness[106]. Therefore, further research is essential to understand these aspects of the compounds present in the ethyl acetate fraction of *C. longa* rhizome and their mechanism of action in the body. Additionally, investigating the long-term effects of EAF treatment and its efficacy in other models of pulmonary toxicity, as well as its potential in combination with other therapeutic agents, is crucial. This will be vital for the development of targeted therapeutic interventions.

4.1 Selection of Suitable Solvent Fraction of *Curcuma longa* for the Ameliorative Potential in Benz[A]Anthracene-induced Pulmonary Toxicity

The selection of a suitable solvent fraction was considered based on the outcome of the comparisons made from the effects of the different solvent fractions of *C. longa Linn* rhizome on benz[a]anthracene-induced toxicity. In the above experiment; the EAF of the *C. longa* rhizome had the highest percentage yield when compared to the ETF, HXF, and DEF fractions. The body weight recovery was higher in the EAF-treated group than in the other treatment groups after 2 weeks of administration and significantly ($p<.05$) increased when compared to the end-of-induction average weight gained. The post-treatment EAF haematologic parameters were relatively normal blood picture which was not significantly ($p>.05$) different from the control and diclofenac-treated groups. The post-treatment serum EGFR and CYFRA 21-1 levels were significantly ($p<.05$) decreased in the EAF-treated group when compared to the post-induction values. There was no significant ($p>.05$) difference in these values when compared to the diclofenac-treated group. The outcome

was different in the ETF, HXF, and DEF-treated groups. The antioxidant activities in the lung tissue of the EAF-treated group were also remarkable because most of the antioxidant activity measured had no significant (p>.05) difference when compared to that of the diclofenac-treated group and the control group. The lung tissue damage in the EAF-treated group was minimal having the lowest score when compared to the other treatment groups and much more minimal when compared to the untreated group.

Summarily, the EAF of *C. longa* rhizome is more capable of reducing cellular damage and oxidative stress following exposure to benz[a]anthracene than HXF, ETF, and DEF.

5. Conclusion

The EAF of *C. longa* rhizome showed promise for therapeutic application in mitigating benz[a]anthracene-induced toxicity, particularly in lung damage. Benz[a] anthracene exposure induced oxidative stress and impaired antioxidant enzyme activities, with EAF showing protective effects. EAF demonstrated the most significant reduction in lung tissue injury induced by benz[a]anthracene, suggesting anti-inflammatory and tissue-protective properties.

6. References

1. Agilent Technologies. Material safety data sheet: Benz[a] anthracene. Available from: https://www.agilent.com/cs/library/msds/P-640-1_NAEnglish.pdf](https://www.agilent.com/cs/library/msds/P-640-1_NAEnglish.pdf
2. Talhout R, Schulz T, Florek E, Van Benthem J, Wester P, Opperhuizen A. Hazardous compounds in tobacco smoke. Int J Environ Res Public Health. 2011; 8(2):613-28. https://doi.org/10.3390/ijerph8020613 PMid:21556207 PMCid: PMC3084482.
3. Gray JP, Hall GJ. Benz [a] anthracene. In: Wexler P, editors. Encyclopedia of Toxicology: 3rd ed. Academic Press; 2014. p. 413-4. https://doi.org/10.1016/B978-0-12-386454-3.00247-5 PMid:25007322.
4. Wallig MA, Bolon B, Haschek WM, Rousseaux CG, editors. Fundamentals of toxicologic pathology. 2nd ed. Academic Press; 2017. p. 93-133.
5. Oluchi OM, Chukwuebuka NH, Orbunde DK, Saganuwan SA, Azubuike OP. Evaluation of Benz [A] anthracene-induced pulmonary toxicity in *Rattus norvegicus*. J Toxicol Environ Health Sci. 2023; 16(1):1-12.
6. Yue GG, Chan BC, Hon PM, Lee MY, Fung KP, Leung PC, Lau CB. Evaluation of *in vitro* anti-proliferative and immunomodulatory activities of compounds isolated from *C. longa*. Food Chem Toxicol. 2010; 48(8-9):2011-20. https://doi.org/10.1016/j.fct.2010.04.039 PMid:20438793 PMCid: PMC2910176.
7. Mathai NJ, Sony D, Mane PP, Shetty CB, Latheef L, Kamath K, Kochikuzhyil BM, Baliga MS. Antiarthritic effects of turmeric and curcumin: A revisit. In: Watson RR, Preedy VR, editors. Polyphenols: Prevention and Treatment of Human Disease. Academic Press; 2018. p. 247-52. https://doi.org/10.1016/B978-0-12-813008-7.00020-5
8. Chanda S, Ramachandra TV. Phytochemical and pharmacological importance of turmeric (*C. longa*): A review. Res Rev: J Pharmacol. 2019; 9(1):16-23.
9. Liju VB, Jeena K, Kuttan R. An evaluation of antioxidant, anti-inflammatory, and antinociceptive activities of essential oil from *C. longa* L. Indian J Pharmacol. 2011; 43(5):526-31. https://doi.org/10.4103/0253-7613.84961 PMid:22021994 PMCid: PMC3195121.
10. Kumar N, Pruthi V. Potential applications of ferulic acid from natural sources. Biotechnol Rep. 2014; 4:86-93. https://doi.org/10.1016/j.btre.2014.09.002 PMid:28626667 PMCid: PMC5466124.
11. He Y, Yue Y, Zheng X, Zhang K, Chen S, Du Z. Curcumin, inflammation, and chronic diseases: how are they linked? Molecules. 2015; 20(5):9183-213. https://doi.org/10.3390/molecules20059183 PMid:26007179 PMCid: PMC6272784
12. Jyotirmayee B, Mahalik G. A review on selected pharmacological activities of *C. longa* L. Int J Food Prop. 2022; 25(1):1377-98. https://doi.org/10.1080/10942912.2022.2082464
13. Malwade CR, Qu H, Rong BG, Christensen LP. Chemometrics for analytical data mining in separation process design for recovery of artemisinin from *Artemisia annua*. Ind Eng Chem Res. 2014; 53(13):5582-9. https://doi.org/10.1021/ie404233z
14. Council for International Organizations of Medical Sciences (CIOMS). International guiding principles for biomedical research involving animals. Altern Lab Anim. 1985; 12:2.
15. Parasuraman S, Raveendran R, Kesavan R. Blood sample collection in small laboratory animals. J Pharmacol Pharmacother. 2010; 1(2):87. https://doi.org/10.4103/0976-500X.72350 PMid:21350616 PMCid: PMC3043327
16. Cheesbrough M. District laboratory practice in tropical countries. Part 1. 2nd ed. Cambridge university press; 2006.
17. Wayne PA. Procedure for determining packed cell volume by the microhematocrit method; Approved Standard-Third Edition. Document H07-A3; 2000.
18. Pal GK. Textbook of practical physiology-2nd Edn. Orient Blackswan; 2006.

19. Wayne PA. Reference leukocyte (WBC) differential count (proportional) and evaluation of instrument methods: Approved standard. Document H20-A2; 2007.
20. Chabot-Richards DS, George TI. White blood cell counts reference methodology. Clin Lab Med. 2015; 35(1):11-24. https://doi.org/10.1016/j.cll.2014.10.007 PMid:25676369
21. Underwood W, Anthony R. AVMA guidelines for the euthanasia of animals: 2020 edition. 2013(30), 2020-1; 2020.
22. Simpson RJ. Homogenization of mammalian tissue. Cold Spring Harbor Protoc. 2010; 2010(7):pdb-prot5455. https://doi.org/10.1101/pdb.prot5455 PMid:20647359.
23. Jollow DJ, Mitchell JR, Zampaglione NA, Gillette JR. Bromobenzene-induced liver necrosis. Protective role of glutathione and evidence for 3, 4-bromobenzene oxide as the hepatotoxic metabolite. Pharmacology. 1974; 11(3):151-69. https://doi.org/10.1159/000136485 PMid:4831804
24. Habig WH, Pabst MJ, Jakoby WB. Glutathione S-transferases: The first enzymatic step in mercapturic acid formation. J Biol Chem. 1974; 249(22):7130-9. https://doi.org/10.1016/S0021-9258(19)42083-8 PMid:4436300
25. Carlberg I, Mannervik B. Purification and characterization of the flavoenzyme glutathione reductase from rat liver. J Biol Chem. 1975; 250(14):5475-80.https://doi.org/10.1016/S0021-9258(19)41206-4 PMid:237922
26. Mohandas J, Marshall JJ, Duggin GG, Horvath JS, Tiller DJ. Differential distribution of glutathione and glutathione-related enzymes in rabbit kidney: Possible implications in analgesic nephropathy. Biochem Pharmacol. 1984; 33(11):1801-180. https://doi.org/10.1016/0006-2952(84)90353-8 PMid:6145422
27. Clairbone A. Catalase activity. In: Handbook of methods for oxygen radical research. Boca Raton (FL): CRC Press; 1985. p. 283-284.
28. Beauchamp C, Fridovich I. Superoxide dismutase: Improved assays and an assay applicable to acrylamide gels. Anal Biochem. 1971; 44(1):276-87. https://doi.org/10.1016/0003-2697(71)90370-8 PMid:4943714
29. Bradford MM. A rapid and sensitive method for the quantitation of microgram quantities of protein utilizing the principle of protein-dye binding. Anal Biochem. 1976; 72(1-2):248-54. https://doi.org/10.1006/abio.1976.9999 PMid:942051
30. Drury RA, Wellington EA. Carlton's histopathological techniques. Oxford: Oxford University Press; 1976.
31. Holland T, Holland C. Analysis of unbiased histopathology data from rodent toxicity studies (or, are these groups different enough to ascribe it to treatment?). Toxicol Pathol. 2011; 39(4):569-75. https://doi.org/10.1177/0192623311406289 PMid:21558466
32. Ashcroft T, Simpson JM, Timbrell V. Simple method of estimating the severity of pulmonary fibrosis on a numerical scale. J Clin Pathol. 1988; 41(4):467-70. https://doi.org/10.1136/jcp.41.4.467 PMid:3366935 PMCid: PMC1141479
33. Hübner RH, Gitter W, Eddine El Mokhtari N, Mathiak M, Both M, Bolte H, *et al.* Standardized quantification of pulmonary fibrosis in histological samples. Biotechniques. 2008; 44(4):507-17. https://doi.org/10.2144/000112729 PMid:18476815
34. Kubiak BD, Albert SP, Gatto LA, Snyder KP, Maier KG, Vieau CJ, *et al.* Peritoneal negative pressure therapy prevents multiple organ injury in a chronic porcine sepsis and ischemia/reperfusion model. Shock. 2010; 34(5):525-34. https://doi.org/10.1097/SHK.0b013e3181e14cd2 PMid:20823698
35. Silva IAN, Gvazava N, Bölükbas DA, Stenlo M, Dong J, Hyllen S, *et al.* A semi-quantitative scoring system for green histopathological evaluation of large animal models of acute lung injury. Bio-Protocol. 2022; 12(16):e4493. https://doi.org/10.21769/BioProtoc.4493 PMCid: PMC9486691
36. Gibson PG, Simpson JL. The overlap syndrome of asthma and COPD: what are its features and how important is it? Thorax. 2009; 64(8):728-35. https://doi.org/10.1136/thx.2008.108027 PMid:19638566.
37. GraphPad Software Inc, La Jolla, CA, USA.
38. Ngo TV, Scarlett CJ, Bowyer MC, Ngo PD, Vuong QV. Impact of different extraction solvents on bioactive compounds and antioxidant capacity from the root of *Salacia chinensis* L. J Food Qual. 2017. https://doi.org/10.1155/2017/9305047
39. Ibrahim HAH. Introductory chapter: Fractionation. In: Fractionation. IntechOpen; 2018.
40. Stéphane FFY, Jules BKJ, Batiha GE, Ali I, Bruno LN. Extraction of bioactive compounds from medicinal plants and herbs. Nat Med Plants. 2021.
41. Arawande JO, Akinnusotu A, Alademeyin JO. Extractive value and phytochemical screening of ginger (*Zingiber officinale*) and turmeric (*C. longa*) using different solvents. Int J Trad Nat Med. 2018; 8(1):13-22.
42. Cui Z, Yao L, Ye J, Wang Z, Hu Y. Solubility measurement and thermodynamic modelling of curcumin in twelve pure solvents and three binary solvents at different temperatures (T= 278.15-323.15 K). J Mol Liquids. 2021; 338:116795. https://doi.org/10.1016/j.molliq.2021.116795
43. Pant P, Pandey S, Dall'Acqua S. The influence of environmental conditions on secondary metabolites in medicinal plants: A literature review. Chem Biodivers. 2021; 18(11):e2100345. https://doi.org/10.1002/cbdv.202100345 PMid:34533273
44. Zhang QW, Lin LG, Ye WC. Techniques for extraction and isolation of natural products: A comprehensive review. Chin Med. 2018; 13:1-26. https://doi.org/10.1186/s13020-018-0177-x
45. Abubakar AR, Haque M. Preparation of medicinal plants: Basic extraction and fractionation procedures for experimental purposes. J Pharm Bioallied Sci. 2020; 12(1):1.

https://doi.org/10.4103/jpbs.JPBS_175_19 PMid:32801594 PMCid: PMC7398001
46. Yuan H, Ma Q, Ye L, Piao G. The traditional medicine and modern medicine from natural products. Molecules. 2016; 21(5):559. https://doi.org/10.3390/molecules21050559 PMid:27136524 PMCid: PMC6273146
47. Nasim N, Sandeep IS, Mohanty S. Plant-derived natural products for drug discovery: Current approaches and prospects. Nucleus. 2022; 65(3):399-411. https://doi.org/10.1007/s13237-022-00405-3 PMid:36276225 PMCid: PMC9579558
48. van Berlo D, Woutersen M, Muller A, Pronk M, Vriend J, Hakkert B. 10% Body weight (gain) change as a criterion for the maximum tolerated dose: A critical analysis. Regul Toxicol Pharmacol. 2022; 134:105235. https://doi.org/10.1016/j.yrtph.2022.105235 PMid:35917983
49. Cederholm T, Barazzoni R, Austin P, Ballmer P, Biolo GIANNI, Bischoff SC, *et al*. ESPEN guidelines on definitions and terminology of clinical nutrition. Clin Nutr. 2017; 36(1):49-64. https://doi.org/10.1016/j.clnu.2016.09.004 PMid:27642056
50. Piao Y, Liu Y, Xie X. Change trends of organ weight background data in Sprague Dawley rats at different ages. J Toxicol Pathol. 2013; 26(1):29-34. https://doi.org/10.1293/tox.26.29 PMid:23723565 PMCid: PMC3620211
51. Silva AV, Norinder U, Liiv E, Platzack B, Öberg M, Törnqvist E. Associations between clinical signs and pathological findings in toxicity testing. ALTEX. 2021; 38(2):198-214. https://doi.org/10.14573/altex.2003311 PMid:33118607
52. Moldoveanu B, Otmishi P, Jani P, Walker J, Sarmiento X, Guardiola J, *et al.* Inflammatory mechanisms in the lung. J Inflamm Res. 2009; 2:1-11.
53. Elshama SS, El-Kenawy AEM, Osman HEH. Histopathological study of cyclosporine pulmonary toxicity in rats. J Toxicol. 2016. https://doi.org/10.1155/2016/2973274 PMid:26941796 PMCid: PMC4749835
54. Ranieri VITO, Rubenfeld GD, Thompson BT, Ferguson ND, Caldwell E, Fan E, *et al*. Acute respiratory distress syndrome: the Berlin Definition. Jama. 2012; 307(23):2526-33. https://doi.org/10.1001/jama.2012.5669
55. Aulbach AD, Amuzie CJ. Biomarkers in nonclinical drug development. In: A comprehensive guide to toxicology in nonclinical drug development. Academic Press; 2017. p. 447-471. https://doi.org/10.1016/B978-0-12-803620-4.00017-7
56. Hussan F, Mansor AS, Hassan SN, Kamaruddin TNE, Tasnim TN, Budin SB, *et al*. The anti-inflammatory property of Plantago major leaf extract reduces the inflammatory reaction in experimental acetaminophen-induced liver injury. Evid Based Complement Alternat Med. 2015. https://doi.org/10.1155/2015/347861 PMid:26300946 PMCid: PMC4537734
57. Peng J. The pharmacological targets and clinical evidence of natural products with anti-hepatic inflammatory properties. Front Pharmacol. 2018; 9:455. https://doi.org/10.3389/fphar.2018.00455 PMid:29922155 PMCid: PMC5996099
58. Jacob Filho W, Lima CC, Paunksnis MRR, Silva AA, Perilhão MS, Caldeira M, *et al*. Reference database of haematological parameters for growing and ageing rats. Ageing Male. 2018; 21(2):145-8. https://doi.org/10.1080/13685538.2017.1350156 PMid:28696817
59. Lowe D, Sanvictores T, Zubair M, John S. Alkaline phosphatase. StatPearls; 2023.
60. Lala V, Zubair M, Minter D. Liver function tests. StatPearls; 2023.
61. Gregus Z, Klaassen CD. Mechanisms of toxicity. The basic science of poisons. 5th ed. New York: McGraw-Hill; 2001. p. 35-74.
62. Everds NE, Snyder PW, Bailey KL, Bolon B, Creasy DM, Foley GL, *et al*. Interpreting stress responses during routine toxicity studies: a review of the biology, impact, and assessment. Toxicol Pathol. 2013; 41(4):560-614. https://doi.org/10.1177/0192623312466452 PMid:23475558
63. Higgins C. Urea and creatinine concentration, the urea: creatinine ratio. Acute Care Test Hand. 2016:1-8.
64. Gounden V, Bhatt H, Jialal I. Renal function tests. StatPearls Publishing; 2023.
65. Catanzaro M, Corsini E, Rosini M, Racchi M, Lanni C. Immunomodulators inspired by nature: A review on curcumin and echinacea. Molecules. 2018; 23(11):2778. https://doi.org/10.3390/molecules23112778 PMid:30373170 PMCid: PMC6278270
66. Yuandani, Jantan I, Rohani AS, Sumantri IB. Immunomodulatory effects and mechanisms of Curcuma species and their bioactive compounds: A review. Front Pharmacol. 2021; 12:643119. https://doi.org/10.3389/fphar.2021.643119 PMid:33995049 PMCid: PMC8120430
67. Behl T, Kumar K, Brisc C, Rus M, Nistor-Cseppento DC, Bustea C, *et al*. Exploring the multifocal role of phytochemicals as immunomodulators. Biomed Pharmacother. 2021; 133:110959. https://doi.org/10.1016/j.biopha.2020.110959 PMid:33197758
68. Morell AR. CEA serum levels in non-neoplastic disease. Int J Biol Markers. 1992; 7(3):160-6. https://doi.org/10.1177/172460089200700307 PMid:1431339
69. Sigismund S, Avanzato D, Lanzetti L. Emerging functions of the EGFR in cancer. Mol Oncol. 2018; 12(1):3-20. https://doi.org/10.1002/1878-0261.12155 PMid:29124875 PMCid: PMC5748484
70. Andhi T, Zubair M, Bhatt H. Cancer Antigen 125. In: StatPearls [Internet]. Treasure Island (FL): StatPearls Publishing; 2023. Available from: https://www.ncbi.nlm.nih.gov/books/NBK562245/

71. Kankanala VL, Mukkamalla SKR. Carcinoembryonic Antigen. In: StatPearls [Internet]. Treasure Island (FL): StatPearls Publishing; 2023. Available from: https://www.ncbi.nlm.nih.gov/books/NBK578172/
72. Pujol JL, Grenier J, Daurès JP, Daver A, Pujol H, Michel FB. Serum fragment of cytokeratin subunit 19 measured by CYFRA 21-1 immunoradiometric assay as a marker of lung cancer. Cancer Res. 1993; 53(1):61-6.
73. Stieber P, Hasholzner U, Bodenmüller H, Nagel D, Sunder-Plassmann L, Dienemann H, *et al.* CYFRA 21-1: A new marker in lung cancer. Cancer. 1993; 72(3):707-13. https://doi.org/10.1002/1097-0142(19930801)72:3<707::AID-CNCR2820720313>3.0.CO;2-X PMid:7687515.
74. Wieskopf B, Demangeat C, Purohit A, Stenger R, Gries P, Kreisman H, *et al.* Cyfra 21-1 as a biologic marker of non-small cell lung cancer: Evaluation of sensitivity, specificity, and prognostic role. Chest. 1995; 108(1):163-9. https://doi.org/10.1378/chest.108.1.163 PMid:7541742.
75. Agency for Toxic Substances and Disease Registry. Toxicological profile for polycyclic aromatic hydrocarbons. Atlanta, GA: ATSDR; 1995.
76. Mumtaz MM, George JD, Gold KW, Cibulas W, DeRosa CT. ATSDR evaluation of health effects of chemicals. IV. Polycyclic Aromatic Hydrocarbons (PAHs): Understanding a complex problem. Toxicol Ind Health. 1996; 12(6):742-971. https://doi.org/10.1177/074823379601200601 PMid:9050165.
77. Sevinc A, Adli M, Kalender ME, Camci C. Benign causes of increased serum CA-125 concentration. Lancet Oncol. 2007; 8(12):1054-5. https://doi.org/10.1016/S1470-2045(07)70357-1 PMid:18054877.
78. Johnson CC, Kessel B, Riley TL, Ragard LR, Williams CR, Xu JL, *et al.* The epidemiology of CA-125 in women without evidence of ovarian cancer in the Prostate, Lung, Colorectal, and Ovarian Cancer (PLCO) Screening Trial. Gynecol Oncol. 2008; 110(3):383-9. https://doi.org/10.1016/j.ygyno.2008.05.006 PMid:18586313 PMCid: PMC3744195.
79. Sang GY, Chen ZY, Meng CR, Tian T, Zhang ZX. Serum tumour marker carbohydrate antigen 125 levels and carotid atherosclerosis in patients with coronary artery disease. Open Medicine. 2018; 13(1):534-8. https://doi.org/10.1515/med-2018-0078 PMid:30613787 PMCid: PMC6310918.
80. Bardelčíková A, Šoltys J, Mojžiš J. Oxidative stress, inflammation and colorectal cancer: An overview. Antioxidants. 2023; 12(4):901. https://doi.org/10.3390/antiox12040901 PMid:37107276 PMCid: PMC10135609.
81. Fukuda I, Yamakado M, Kiyose H. Influence of smoking on serum carcinoembryonic antigen levels in subjects who underwent multiphasic health testing and services. J Med Syst. 1998; 22(2):89-93. https://doi.org/10.1023/A:1022643102208 PMid:9571515.
82. Thomas P, Forse RA, Bajenova O. Carcinoembryonic Antigen (CEA) and its receptor hnRNP M are mediators of metastasis and the inflammatory response in the liver. Clin Exp Metastasis. 2011; 28:923-32. https://doi.org/10.1007/s10585-011-9419-3 PMid:21901530.
83. Rizeq B, Zakaria Z, Ouhtit A. Towards understanding the mechanisms of actions of carcinoembryonic antigen-related cell adhesion molecule 6 in cancer progression. Cancer Sci. 2018; 109(1):33-42. https://doi.org/10.1111/cas.13437 PMid:29110374 PMCid: PMC5765285
84. Kwon YJ, Lee HS, Shim JY, Lee YJ. Serum carcinoembryonic antigen is positively associated with leukocyte count in Korean adults. J Clin Lab Anal. 2018; 32(3):e22291. https://doi.org/10.1002/jcla.22291 PMid:28653772 PMCid: PMC6817189
85. Hodges RE, Minich DM. Modulation of metabolic detoxification pathways using foods and food-derived components: A scientific review with clinical application. J Nutr Metab. 2015; 2015:760689. https://doi.org/10.1155/2015/760689 PMid:26167297 PMCid: PMC4488002.
86. Lee JH, Lee SW. The roles of carcinoembryonic antigen in liver metastasis and therapeutic approaches. Gastroenterol Res Pract. 2017. https://doi.org/10.1155/2017/7521987 PMid:28588612 PMCid: PMC5447280.
87. Li Y, Cao H, Jiao Z, Pakala SB, Sirigiri DNR, Li W, *et al.* Carcinoembryonic antigen interacts with the TGF-β receptor and inhibits TGF-β signalling in colorectal cancers. Cancer Res. 2010; 70(20):8159-68. https://doi.org/10.1158/0008-5472.CAN-10-1073 PMid:20889724 PMCid: PMC3001246.
88. Huang R, Meng T, Zha Q, Cheng K, Zhou X, Zheng J, *et al.* The predicting roles of carcinoembryonic antigen and its underlying mechanism in the progression of coronavirus disease 2019. Crit Care. 2021; 25(1):1-20. https://doi.org/10.1186/s13054-021-03661-y PMid:34217339 PMCid: PMC8254455.
89. Sharma R, Yang Y, Sharma A, Awasthi S, Awasthi YC. Antioxidant role of glutathione S-transferases: Protection against oxidant toxicity and regulation of stress-mediated apoptosis. Antioxid Redox Signal. 2004; 6(2):289-300. https://doi.org/10.1089/152308604322899350 PMid:15025930.
90. Allocati N, Masulli M, Di Ilio C, Federici L. Glutathione transferases: Substrates, inhibitors, and pro-drugs in cancer and neurodegenerative diseases. Oncogenesis. 2018; 7(1):8. https://doi.org/10.1038/s41389-017-0025-3 PMid:29362397 PMCid: PMC5833873.
91. Chaudhary P, Janmeda P, Docea AO, Yeskaliyeva B, Abdull Razis AF, Modu B, *et al.* Oxidative stress, free radicals and antioxidants: potential crosstalk in the pathophysiology of

human diseases. Front Chem. 2023; 11:1158198. https://doi.org/10.3389/fchem.2023.1158198 PMid:37234200 PMCid: PMC10206224.

92. Alrawaiq NS, Abdullah A. A review of antioxidant polyphenol curcumin and its role in detoxification. Int J Pharm Tech Res. 2014; 6(1):280-9.
93. Fuloria S, Mehta J, Chandel A, Sekar M, Rani NNIM, Begum MY, *et al.* A comprehensive review on the therapeutic potential of *C. longa* Linn. about its major active constituent curcumin. Front Pharmacol. 2022; 13:820806. https://doi.org/10.3389/fphar.2022.820806 PMid:35401176 PMCid: PMC8990857.
94. Lubos E, Loscalzo J, Handy DE. Glutathione peroxidase-1 in health and disease: from molecular mechanisms to therapeutic opportunities. Antioxid Redox Signal. 2011; 15(7): 1957–1997. https://doi.org/10.1089/ars.2010.3586
95. Birben E, Sahiner UM, Sackesen C, Erzurum S, Kalayci O. Oxidative stress and antioxidant defense. World Allergy Organ J. 2012; 5(1):9-19. https://doi.org/10.1097/WOX.0b013e3182439613 PMid:23268465 PMCid: PMC3488923
96. Ighodaro OM, Akinloye OA. First-line defence antioxidants-superoxide dismutase (SOD), catalase (CAT), and glutathione peroxidase (GPX): Their fundamental role in the entire antioxidant defence grid. Alexandria J Med. 2018; 54(4):287-93. https://doi.org/10.1016/j.ajme.2017.09.001
97. Sarıkaya E, Doğan S. Glutathione peroxidase in health and diseases. In: Glutathione system and oxidative stress in health and disease; 2020. https://doi.org/10.5772/intechopen.91009
98. Demirci-Cekic S, Özkan G, Avan AN, Uzunboy S, Çapanoğlu E, Apak R. Biomarkers of oxidative stress and antioxidant defence. J Pharm Biomed Anal. 2022; 209:114477. https://doi.org/10.1016/j.jpba.2021.114477 PMid:34920302.
99. Eteng O, Moses CA, Enobong J, Akamo AJ, Akinloye DI, Ugbaja RN, *et al.* Protective effects of *C. longa* rhizomes ethyl acetate extract against alcohol-induced oxidative stress and nephrotoxicity in female Wistar rats. Asian J Nat Prod Biochem. 2020; 18(1). https://doi.org/10.13057/biofar/f180102
100. Auychaipornlert S, Lawanprasert PP, Piriyaprasarth S, Sithisarn P, Mangmool S. Design of turmeric rhizome extract nano-formula for delivery to cancer cells. Molecules. 2022; 27(3):896. https://doi.org/10.3390/molecules27030896 PMid:35164159 PMCid: PMC8838412
101. Couto N, Wood J, Barber J. The role of glutathione reductase and related enzymes on cellular redox homeostasis network. Free Radic Biol Med. 2016; 95:27-42. https://doi.org/10.1016/j.freeradbiomed.2016.02.028 PMid:26923386
102. Memarzia A, Khazdair MR, Behrouz S, Gholamnezhad Z, Jafarnezhad M, Saadat S, *et al.* Experimental and clinical reports on anti-inflammatory, antioxidant, and immunomodulatory effects of *C. longa* and curcumin, an updated and comprehensive review. BioFactors. 2021; 47(3):311-50. https://doi.org/10.1002/biof.1716 PMid:33606322
103. Bansal M, Poonia A, Kolluri SRP, Vasundhara. Introduction on bioactive compounds, sources, and their potential applications. In: Bansal M, Poonia A, Kolluri SRP, Vasundhara, editors. Bioactive Components: A sustainable system for good health and well-being. Singapore: Springer Nature Singapore; 2022. p. 3-26. https://doi.org/10.1007/978-981-19-2366-1_1 PMCid: PMC10081712